Current Scenario of Nanocomposite Materials for Fuel Cell Applications

Raveendra M. Hegde, Mahaveer D. Kurkuri and Madhuprasad Kigga

List of Abbreviations

FC	Fuel cell
PEM	Proton exchange membrane
PEMFC	Proton exchange membrane fuel cell
AFC	Alkaline fuel cell
DMFC	Direct methanol fuel cell
PAFC	Phosphoric acid fuel cell
MCFC	Molten carbonate fuel cell
SOFC	Solid oxide fuel cell
MEA	Membrane electrode assembly
GDL	Gas diffusion layers
RH	Relative humidity
PEEK	Poly (ether ether ketone)
SPEEK	Sulfonated poly (ether ether ketone)
PBI	Polybenzimidazole
PVA	Polyvinyl alcohol
ORR	Oxygen reduction reaction
CV	Cyclic voltammetry
XRD	X-ray diffraction
DFT	Density functional theory
PECVD	Plasma enhanced chemical vapor deposition
CNT	Carbon nanotubes
SWCNT	Single-walled carbon nanotubes
MWCNT	Multi-walled carbon nanotubes
IEC	Ion exchange capacity

R. M. Hegde · M. D. Kurkuri (✉) · M. Kigga (✉)
Centre for Nano and Material Sciences, Jain University, Jain Global Campus,
Bengaluru 562 112, Karnataka, India
e-mail: mahaveer.kurkuri@jainuniversity.ac.in

M. Kigga
e-mail: madhuprasad@jainuniversity.ac.in

Inamuddin et al. (eds.), *Sustainable Polymer Composites and Nanocomposites*,
https://doi.org/10.1007/978-3-030-05399-4_20

1 Introduction

The increasing population and rapid urbanization are leading to a sudden rise in the energy consumption worldwide. To fulfil this huge demand, fossil fuels have been extensively exploited as a major source of energy until date. However, this source of energy consumption is creating irreversible damage to the environment by producing huge and rapid carbon footprint and hence constant depletion of this source is eventually leading to the energy crisis in most of the countries today [1]. In addition, it has been predicted that there will be more than 50% increase in energy demand by next 25 years, which cannot be met just by relying majorly on fossil fuel source. Therefore, exploring the alternative energy sources have become inevitable in fulfilling the energy demand of future generation. Consequently, renewable energy sources, on the other hand, are promising sources of energy and are very fast developing technology as it provides the energy with significantly less pollution. Though several alternative technologies such as solar, wind, tidal, biomass have been developed, they all have been restricted for complete commercial exploitation because of their drawbacks such as storage issues, energy conversion, efficiency, transportation etc. Consequently, fuel cells (FCs) are considered to be a future source of energy to meet the rising energy demand and thus, have been attracting the wide scientific community to develop sustainable technology for efficient energy generation [2]. It is an emerging field of research in energy materials as it provides clean and green energy source with a conversion efficiency as high as 60%. Contrasting to other electrochemical sources like batteries, FCs requires the constant supply of fuel and oxygen to retain the continuous electrochemical reaction process, whereas, in a battery, the previously loaded chemicals in a batch process format attain the energy. However, FCs obtain the energy sources continuously from the exterior of the cell i.e., hydrogen from the fuel and oxygen from the environment [3]. Also, the possibilities of rapid recharging, off-grid operations, a significant reduction in weight, noise-free operations are the added advantages with FCs. More importantly, FCs reduce the greenhouse gas emission and produce only water as the main by-product. Therefore, it is significantly applied in portable energy devices, automobiles, transportation vehicles [4]. However, the conditions like high-temperature operation, availability of fuel source and infrastructures are hindering the further development of FCs and their usage in large scale.

1.1 Working Principle of FC

FCs are the galvanic cells, which work on the principle of oxidation and reduction reactions at the anode and cathode respectively. They use hydrogen or hydrogen-rich fuels for electrochemical reactions as hydrogen contains high energy per unit weight than any other fuels. A conventional FC is illustrated in Fig. 1

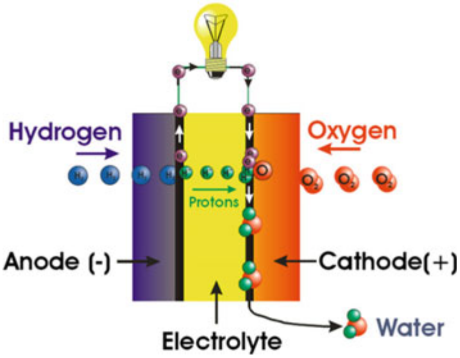

Fig. 1 Schematic representation of a conventional fuel cell. Reproduced with permission from Ref. [5], Copyright 2010, Elsevier

which consists of a sandwiched membrane between the anode, cathode, and electrolyte by forming a membrane electrode assembly (MEA) along with gas diffusion layers (GDL).

The electrochemical reactions are involving the continuous oxidation of hydrogen at anode and reduction of oxygen at the cathode. This chemical reaction produces the electrons, which are opposed by the electrolytic membrane and they move through an external circuit to produce direct current. The reactions involved in FCs are given below;

$$\text{At anode: } 2H_2 \rightarrow 4H^+ + 4e^-$$
$$\text{At cathode: } O_2 + 4H^+ + 4e^- \rightarrow 2H_2O$$
$$\text{Overall reaction: } 2H_2 + O_2 \rightarrow 2H_2O$$

To dissociate the hydrogen fuel into constituent ions, the FCs are equipped with the catalyst at the anode. Generally, platinum is most widely used as anode catalyst as it exhibits highest electrocatalytic activities in organic fuel redox reactions. The outer layer of catalyst is constructed with GDL, which promotes the transfer of reactants into catalyst layer and helps in the removal of by-product, water. GDL is composed of a thick porous array of carbon fibers, which provides a conductive pathway for current collection. Further, GDL also helps in the electronic connection between bipolar plate and electrode through the channel of MEA. In addition, GDL enhances the mechanical strength of MEA and protects the catalyst layer from corrosion.

The amount of total current produced by the FC depends on cell size, type of the cell, operating temperature and extent of gaseous pressure applied to it. During the electrochemical reactions, FC produces only a small amount of current in the range of 0.6–0.87 V. Therefore, in order to obtain a high voltage, a parallel or series of single cells are constructed as illustrated in Fig. 2. Further, each FC in a stack is separated by a bipolar plate which assists in the uniform distribution of fuel and oxygen in MEA. Polymer-based gaskets are inserted around the edges of MEA to

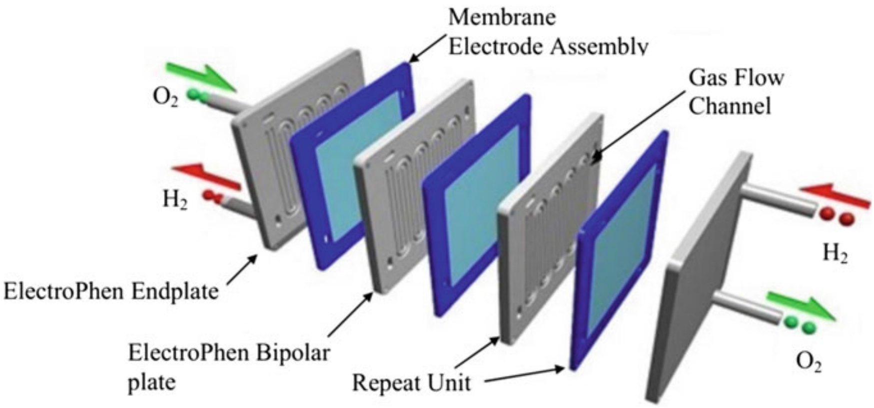

Fig. 2 Schematic representation for the construction of fuel cell stack. Reproduced from Ref. [6], Copyright 2013, Bentham Open

strengthen the FC stack as it is much effective in holding the MEA and adjusting the required pressure inside the system. The produced current is collected by a collector plate which is presented at the terminal part of MEA.

1.2 Proton Conduction Mechanism in FC

Proton conduction across the electrolyte membrane is the prime requirement to attain high current density and it is, therefore, efficiency determining a factor for the FC. This proton conduction depends on the modification made to the membrane, extent of sulfonation, relative humidity (RH), and temperature. The proton conduction phenomena generally follow either Grotthuss mechanism or Vehicle mechanism [7]. In Grotthuss mechanism, proton jumps from one ionic site to another through hydrogen bond network (Fig. 3a). For example, in Nafion® membranes, a proton hops from sulfonic acid (SO_3H) site to the nearby acceptor site i.e., water molecule which has potential for proton movement throughout the membrane.

On the other hand, according to the vehicle mechanism (or en masse diffusion mechanism), proton transfer takes place by the diffusion of carrier species in the form of hydrated ions in the electrolyte (Fig. 3b). Here the protons attach itself to the acceptor molecule and thus acceptor molecule moves from one end to another leading to the proton movement across the membrane. Both the above mechanisms depend on the nature and properties of nanocomposites membrane used in the FC. Moreover, the proton conductivity increases with RH of the system due to the presence of more hydrated protons in the system. Therefore, the proposed models can be used to design the suitable organic and inorganic fillers for polymeric membranes compared to pure polymer membranes [9].

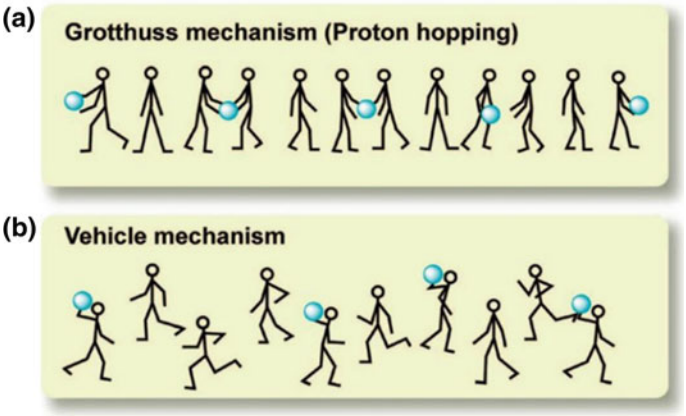

Fig. 3 Schematic representation of **a** Grotthuss mechanism and **b** Vehicle mechanism. Reproduced with permission from Ref. [8], Copyright 2008, American Chemical Society

FCs are generally classified based on the nature of electrolyte used in the cell, operating temperature and types of fuel/oxidants used. Different types of FCs with their properties, efficiency and operating temperature are listed in Table 1.

2 Nanocomposites in FC

To overcome the problems associated with low proton conduction, low current density, fuel crossover, carbon monoxide (CO) poisoning in conventional FCs, in the recent years a new variety of organic, inorganic and polymer-based nanocomposites have been developed. Nanocomposites are hybrid materials with conventional components in it [10, 11] which would be the solution for some of the challenges by providing improved water retention capacity, high energy conversion, and suppression of fuel crossover. Modification of FC composites with organic and inorganic materials is a growing technology in energy material development. Nanomaterials have been integrated with polymers to enhance their original characteristics such as thermal and chemical stabilities [12, 13]. This is attributed to the strong interfacial interaction between the polymers and inserted material. Preparation method of the nanocomposite is one of the important factors in the improvement of FCs as it alters the microstructure of the membranes [14]. Nanomaterials with conventional composite materials have specific properties such as high surface area, specific functional groups, interaction capacity [15–22] that would increase the catalytic performance of the electrodes in FC in terms of rigidity and thermal stability. On the other hand, organic nanocomposites such as sulfonated poly (ether ether ketone) (SPEEK) and polybenzimidazole (PBI) have provided the high flexibility, durability, and processability to the components of the FC [23]. The different types of potential nanocomposites and its applications in FC are described

Table 1 Types of important fuel cells and comparison of their properties

Type of fuel cell	Electrolyte	Charge carrier	Anode reaction	Cathode reaction	Overall reaction	Working temperature (°C)	Efficiency (per cell) [%]	Applications
Proton Exchange Membrane Fuel Cell (PEMFC)	Polymer membrane	H^+	$2H_2 \rightarrow 4H^+ + 4e^-$	½ $O_2 + 4H^+ + 4e^- \rightarrow 2H_2O$	$2H_2 + ½\ O_2 \rightarrow 2H_2O$	60–120	50–70	Transportation, military
Alkaline Fuel Cell (AFC)	Aqueous alkaline solution	OH^-	$2H_2 + 4OH^- \rightarrow 4H_2O + 4e^-$	$O_2 + 4e^- + 2H_2O \rightarrow 4OH^-$	$2H_2 + O_2 \rightarrow 2H_2O$	<80	60–70	Transportation, space
Direct Methanol Fuel Cell (DMFC)	Polymer membrane	H^+	$CH_3OH + H_2O \rightarrow CO_2 + 6H^+ + 6e^-$	3/2 $O_2 + 6H^+ + 6e^- \rightarrow 3H_3O$	CH_2OH + 3/2 $O_2 \rightarrow CO_2 + 2H_2O$	60–120	20–30	Transportation, energy storage systems
Phosphoric Acid Fuel Cell (PAFC)	Molten phosphoric acid	H^+	$2H_2 \rightarrow 4H^+ + 4e^-$	O_2 $(g) + 4H^+ + 4e^- \rightarrow 2H_2O$	$2H_2 + O_2 \rightarrow 2H_2O$	150–200	55	Thermal energy consuming system, air conditioning system
Molten Carbonate Fuel Cell (MCFC)	Molten alkaline carbonate	CO_3^{2-}	$H_2 + CO_3^{2-} \rightarrow H_2O + CO_2 + 2e^-$	½ $O_2 + CO_2 + 2e^- \rightarrow CO_3^{2-}$	H_2 + ½ $O_2 + CO_2 \rightarrow H_2O + CO_2$	600–650	55	Combined heat and power for decentralized systems and transportation
Solid Oxide Fuel Cell (SOFC)	Solid ceramic electrolyte (Yttrium stabilized zirconia)	O^{2-}	$H_2 + O_2^- \rightarrow H_2O + 2e^-$	$½\ O_2 + 2e^- \rightarrow O_2^-$	$H_2 + ½\ O_2 \rightarrow 2H_2O$	800–1000	55	Combined heat and power units, uninterruptible power systems (UPS), Primary power units

in the following section. Furthermore, the efficient working of FC by the integration of various nanocomposite materials for the anode, cathode, and hybrid membranes are summarized below.

2.1 Nafion®- Metal Oxide-Based Nanocomposite

Nafion® is a fluoropolymer which is comprised of sulfonated tetrafluoroethylene backbone and it has been extensively using in the development of FC especially the PEMFC due to its excellent proton conductivity. The proton on sulfonic acid can jump from one site to another through Grotthuss mechanism which makes them conduct protons easily and thus, prevents the electron conduction. However, the property of becoming dehydrated at high temperature, high cost and high fuel crossover of Nafion® made its applications in FC limited to a certain extent. Therefore, the modification of Nafion® with other nanomaterials to overcome these drawbacks has gained significant importance.

Recently, Nafion® modified with phosphonate and sulfonate silica nanoparticles (NIM_PO_3 and NIM_SO_3) for high proton conduction was reported [24]. The synthesized nanocomposite membrane (Fig. 4) revealed the excellent proton conducting property even at a low relative humidity and elevated temperature greater than 80 °C. The conductivity of sulfonate-based nanocomposites at 130 °C and 30% RH was 50 mS/cm. The NIM_SO_3 membranes also exhibited the promotion of water retention capacity by increasing the water uptake 32 (± 2) wt% and better mechanical stiffness even above the temperature of 200 °C.

Mohammadi et al. fabricated the Nafion® with metal oxide nanoparticles for PEMFC [25]. They recast the commercial Nafion® with 75 nm sized TiO_2/ZrO_2 nanoparticles by sol-gel and blending method respectively. Nafion®/ZrO_2 nanocomposite membrane offered good proton conduction and with an increase in the concentration of ZrO_2 and Nafion®/TiO_2 membrane displayed a better water retention capacity than Nafion® membranes modified by other conventional methods. Further, these membranes also unveiled the highest PEMFC performance

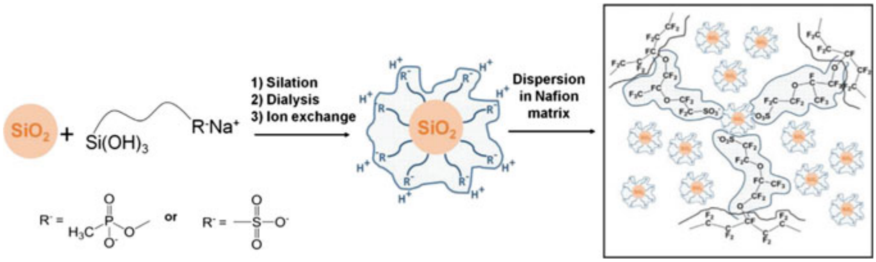

Fig. 4 Schematic representation of the synthesis of Nafion® membranes functionalized with phosphonate and sulfonate nanoparticles. Reproduced with permission from Ref. [24], Copyright 2016, Elsevier

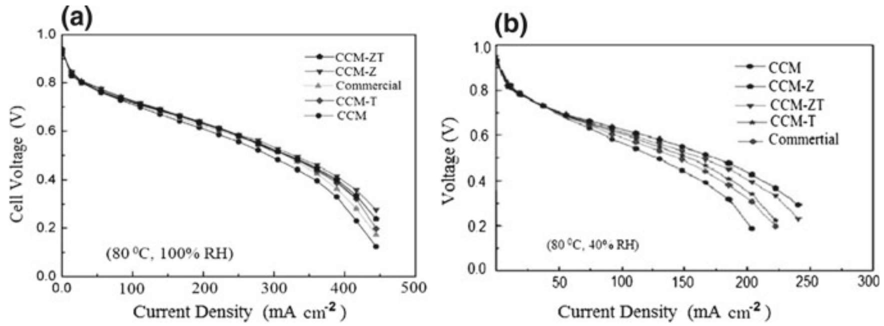

Fig. 5 Comparison of the polarization curves for modified composite membranes and Nafion® membranes at 110 °C, **a** 100% RH, **b** 30% RH. Reproduced with permission from Ref. [25], Copyright 2013, Elsevier

with respect to 1–5 polarization under 110 °C, 0.6 V and 30% RH at 1 atm (Fig. 5). Thus, they proved to be the best-modified membranes for PEMFC.

Integration of Fe_2TiO_5 in Nafion® membranes prepared in water, ethanol and water-ethanol solvent increased proton exchange capacity in FCs [26]. The comparison of the efficiency of membranes revealed that the modified membranes prepared in water solvents are superior to the membranes prepared in either of the solvents. This was due to the fact that water being a polar solvent led the nanoparticles into microscopic swelling and offered strong hydrogen bond whereas, the less polar solvent ethanol couldn't make that to happen. The proton conductivity of 226 mS/cm was obtained by the insertion of 2% Fe_2TiO_5 in commercial Nafion® membrane using water, ethanol and water-ethanol solvents. In addition, the membrane also showed a better water uptake capacity due to the hydrophilic nature of nanoparticles summarized (Table 2).

Table 2 Properties of solvent uptake and proton conduction in Nafion® and modified nanocomposite membranes at 25 °C (95% RH) and 110 °C (70% RH)

Sample code	Thickness (μm)	Solvent uptake (%)	Proton conductivity (mS/cm)	
			25 °C	110 °C
NH-2[a]	231	33	226	240
NHE-2[a]	226	25	87	93
NE-2[a]	240	35	72	80
N[a]	224	22	21	24
N[b]	230	29	6	–
N[c]	238	31	1	–

Reproduced with permission from Ref. [26], Copyright 2014, Elsevier

[a] Membranes stored in water solvent

[b] Membranes stored in a mixture of water-ethanol solvent

[c] Membranes stored in pure ethanol solvent

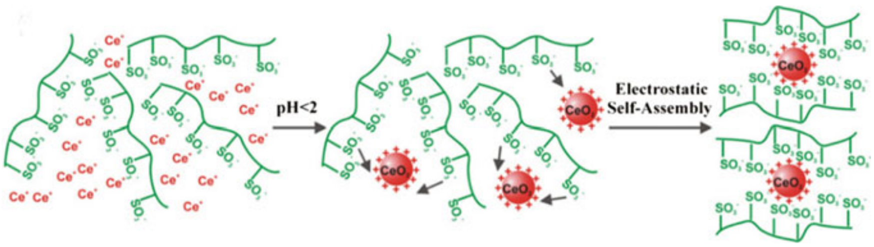

Fig. 6 Graphical representation of self-assembled Nafion®/CeO_2 nanocomposites. Reproduced with permission from Ref. [27], Copyright 2012, Elsevier

The Nafion®/CeO_2 membranes are proved to be the better nanocomposite materials for FC applications. Zhao and co-workers prepared a self-assembly of Nafion®/CeO_2 for electrolyte membrane between positively charged CeO_2 nanoparticle with negatively charged SO_3^- group of Nafion® as illustrated in Fig. 6 [27]. The hybrid nanocomposite membranes were displayed the superior proton exchange capacity and dimensional stability than pristine Nafion® membrane below the RH of 75% and low fluoride emission rate. In addition, the prepared nanocomposite membrane showed a very low fluoride emission rate of 43.05, 8.67, 6.01, and 4.47 mg/h for 1, 3, 5 and 10 wt% the CeO_2, respectively. However, the pristine Nafion® membrane showed 55.78 mg/h and 11.64 mg/h by the same Nafion® membrane synthesized by a sol-gel process. The material also exhibited the irreversible open reduction rate of 1.13×10^{-4} mV/s which was much lower than pristine Nafion® membrane (5.78×10^{-4} mV/s) and the Nafion® membrane prepared through sol-gel method (5.78×10^{-4} mV/s).

Cozzi and co-workers [28] modified the pristine Nafion® with propyl sulfonic (RSO_3H) acid on TiO_2 nanoparticles (TiO_2–RSO_3H) to achieve a higher efficiency in IEC and proton conductivity. The synthesis of TiO_2–RSO_3H is illustrated in Fig. 7. The covalently grafted hybrid materials as a nanocomposite with Nafion® promoted the efficiency of DMFC. The conductivity value of this material obtained was 80 mS/cm at 140 °C at the composition of 10 wt% TiO_2–RSO_3H in a single

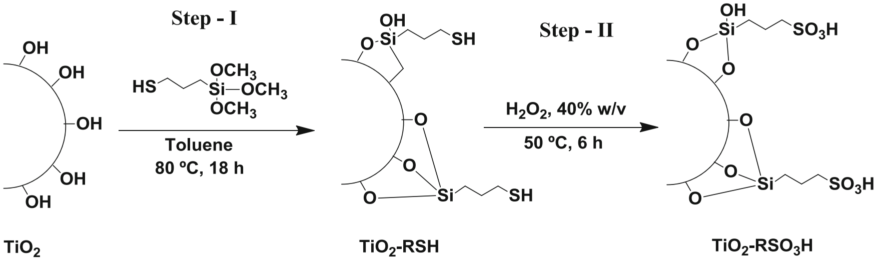

Fig. 7 Functionalization of TiO_2 nanoparticles with propyl sulfonic acid. Reproduced with permission from Ref. [28], Copyright 2014, Elsevier

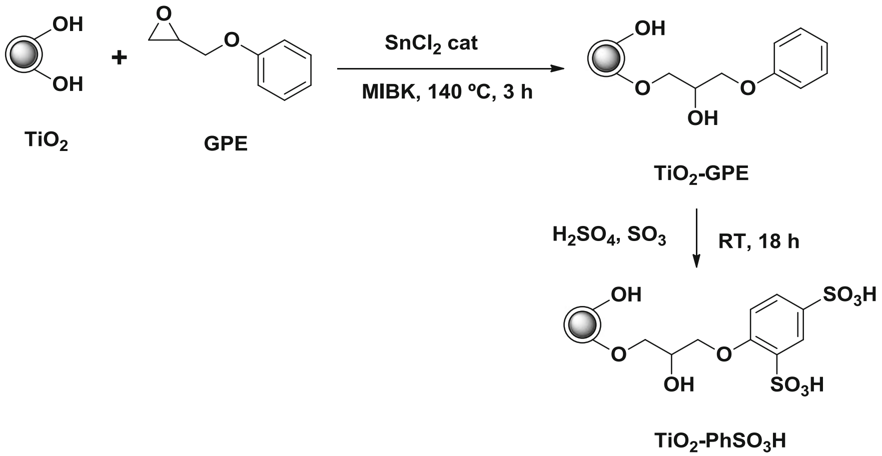

Fig. 8 Functionalization of TiO_2 nanoparticles with phenyl sulfonic acid. Reproduced with permission from Ref. [29], Copyright 2014, Elsevier

cell of DMFC. Also, they showed a supreme power density of 64 mW/cm^2 which is about 40% more than the pristine Nafion® composite membrane.

The organic functionalization of TiO_2 with phenyl sulfonic groups was able to overcome the less proton conduction in FC [29]. Further, the grafting of glycidyl phenyl ether group on the oxide surface was confirmed (Fig. 8) and the IEC was increased due to the covalently bound phenyl sulfonic group. The experimental observation showed that the prepared hybrid membranes reached the highest conductivity of 110 mS/cm at 140 °C with the concentration of 10 wt% TiO_2–$PhSO_3H$. The material also showed the better properties such as reduced methanol crossover (up to 20%) compared to the unfilled Nafion® membrane.

2.2 Graphene-Based Nanocomposites

Graphene has typical properties such as high surface area, surface active sites, electrical conductivity, excellent mechanical strength, high chemical stability and low metal loading capacity. Therefore, it is used for varieties of applications such as electronic devices, energy storage [30–32], sensors and biomedical applications [33]. In addition, the graphene is being used as a supporting material due to the presence of epoxy groups and carboxylic acid groups enhances the proton conducting capacity of the material with metal electrocatalysts for oxygen reduction reaction in FCs [34]. In addition, the stability of nano-catalysts can be increased by dispersing the metal on graphene [35].

The synthetic methods for the preparation of doped graphene and graphene supported nano electrocatalysts with respect to their structure-dependent properties and further developments were discussed by Liu et al. [36]. They have summarized the synthesis and characterization of graphene nanocomposites with various metals electrocatalysts for cathode and anode materials of FC. They elucidated the components into various types i.e. (1) graphene supported metal-free electrocatalysts for high oxygen reduction reaction (ORR) in acid and alkaline electrolytic medium. (2) graphene supported non-noble metals for efficient electrocatalysts (3) graphene-based Pt-free electrocatalysts and alloy nanomaterial for low-cost FC material (4) graphene-supported Pt-based nano-catalysts for increased ORR in electrolytes. These materials were found to participate in the electrooxidation of organic molecules at the anode of Direct Methanol Fuel Cells (DMFC) and ORR at the cathode. By the experimental observation, graphene or co-doped graphene with N, S, B, and P are found to be an excellent cost-effective cathode catalyst for FC applications.

Considering the advantages of graphene, Huang and co-workers developed a novel graphene nanoplate-Pt (GNP/Pt) composite electrocatalysts to obtain the high-performance DMFC [37]. They synthesized a series of graphene nanoplate (GNP/Pt), reduced graphene oxide nanoplate (RGO/Pt) and Vulcan XC-72 Pt (XC-72/Pt) with 0.17 mL of 0.45 M $Pt(NO_3)_2$ as demonstrated in Fig. 9. Further, its electrochemical activity was measured through cyclic voltammetry (CV) and the X-ray diffraction (XRD) patterns which revealed that the Pt was uniformly dispersed over the graphene nanoplates and confirmed the formation of an intact composite. This reduced the probable catalytic poisoning due to methanol oxidation and thus electrocatalytic activity was increased. The time required to increase the electrode potential was significantly decreased in the order of GNP/Pt (~130 s) followed by RGO/Pt (50 s) and XC-72/Pt (~30 s). Thus, they concluded that the GNP/Pt was superior for electrocatalytic activity than RGO/Pt and XC-72/Pt. Also, it is worth in mentioning that GNP can be used as the best catalyst supports for DMFC.

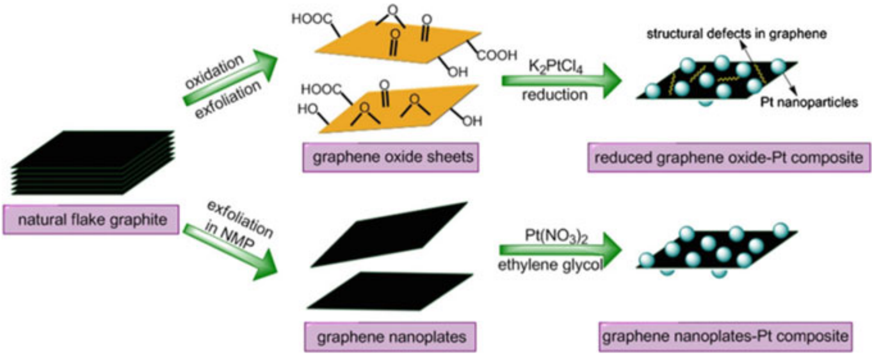

Fig. 9 Illustrations of the synthesis of reduced graphene oxide-Pt composite and graphene nanoplate-Pt composite by the traditional oxidation-reduction method and soft chemical method, respectively. Reproduced with permission from Ref. [37], Copyright 2012, Elsevier

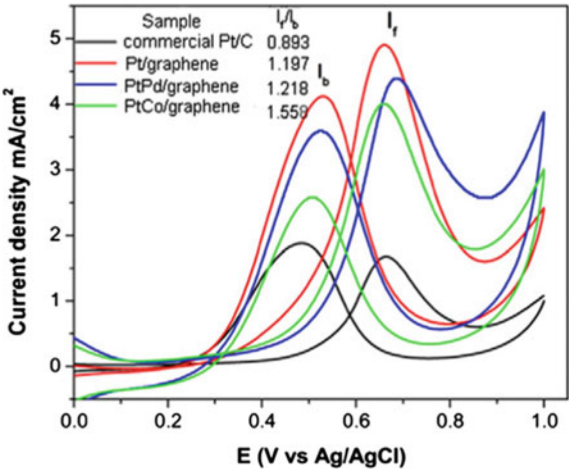

Fig. 10 A comparison of cyclic voltammograms in 0.5 M CH_3OH/0.5 M $HClO_4$ electrolyte at a scanning rate of 50 mV/s displayed by modified materials to evaluate the methanol oxidation and tolerance to CO poisoning. Reproduced with permission from Ref. [38], Copyright 2013, Elsevier

The application of exfoliated graphene-supported Pt and Pt-based alloys as electrocatalysts were elucidated to enhance the performance of DMFC [38]. A low cost and environment-friendly method of “Thermal Expansion and Liquid Exfoliation Solvothermal Reaction (TELESR)” was used to hybridize the exfoliated graphene sheets to load the Pt metal and alloys such as Pt/Pd, Pt/Co nano-clusters. This method improved the methanol oxidation in FC by increasing the electro-catalytic activity. The methanol oxidation was found to be I_f/I_b = 1.218 and 1.558 in PtPd/graphene and PtCo/graphene respectively during an electrochemical analysis. Also, the modified material showed high conductivity and tolerant to carbon monoxide poisoning (Pt/graphene, I_f/I_b = 1.197) compared to commercial Pt/C catalyst (I_f/I_b = 0.893) as shown in Fig. 10. This was due to the interaction of graphene with Pt electronic environment occurred and graphene played a major role in controlling the electronic environment with attached Pt atom which was confirmed by Density Functional Theory (DFT) studies. Therefore, the reported process gives a novel hybridized material that could save the extensive use of expensive Pt metal as electrocatalysts in FC with the increase in performance when compared to conventional Pt/C electrocatalysts for methanol oxidation.

Recently, Nafion®-graphene oxide (GO-Nafion®) nanohybrids for the conduction of high amount protons in PEMFC were described [39]. The reaction of a chain of well-known fluoropolymer, Nafion® onto the GO via Atom Transfer Radical Addition (ATRA) between C-F group of Nafion® and C=C groups of GO presented a nanocomposite material as depicted in Fig. 11.

These nanohybrids form the proton conducting fields by the aggregation of sulfonic acid units of Nafion® material which increases the interfacial compatibility with Nafion® matrix. From the electrochemical analysis, it was evident that the developed nanohybrids showed 1.6 folds high performance in conducting the protons compared to the commercially available Nafion® 112 membranes which

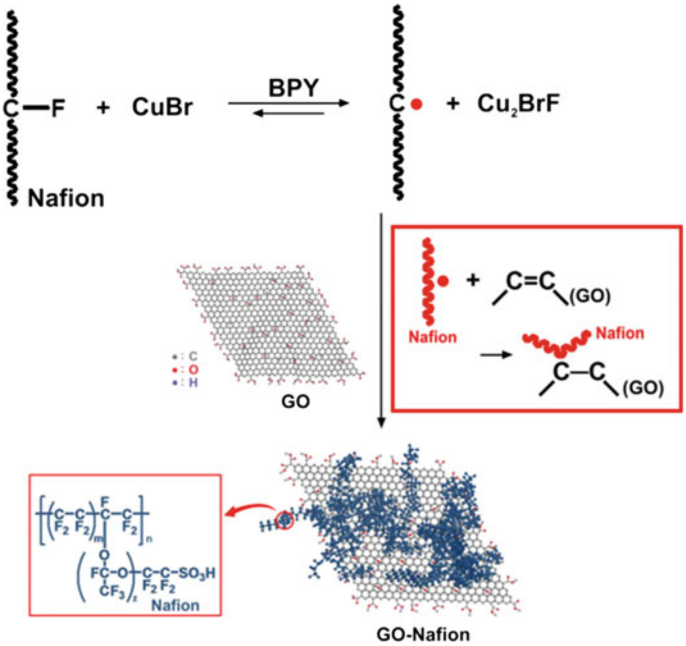

Fig. 11 Schematic representation of the reaction between Nafion® chains onto GO surfaces through an atom transfer radical addition reaction to prepare GO-Nafion® hybrid material. Reproduced with permission from Ref. [39], Copyright 2016, Elsevier

have been summarized in Table 3. Thus, a new variety of material which can be used as nano additive in the fabrication of Nafion® based nanocomposite for the PEM for FC was displayed.

A transition metal hierarchical porous N-doped graphene foams (HPGFs) were prepared by using silica nanoparticles as a template were reported by Zhou and co-workers [40]. The material exhibited the excellent property of ORR in 0.1 M KOH solution with high onset potential of 1.03 V and the limiting current of ~9 mA/cm^2 which was 1.7 times higher than the commercial Pt/C catalyst. Also, an excellent catalytic performance in acidic medium with an onset potential of 0.81 V and the limiting current was up to ~10 mA/cm^2 (Table 4) was observed. Further, the material also showed good methanol tolerance, long-term durability in both acidic and basic conditions. Such excellent material is a model for the development of applied energy systems such as FCs and metal-air batteries.

Nitrogen-doped graphene sheets prepared through plasma enhanced chemical vapour deposition (PECVD) method were studied as anode material for a Microbial Fuel Cell (MFC) [41]. The doping of nitrogen affected the electronic conductivity and catalytic activity due to the formation of structural defects. The material performed with excellent electrocatalytic activity towards glucose oxidation mediated via *Escherichia coli* due to the adjacent contact between microorganism and

Table 3 Proton conduction and single cell performance among various modified GO-Nafion® nanocomposite [39]

Membrane (with % of GO)	Proton conductivity (mS/cm)		Single cell tests					
			H_2/O_2			H_2/air		
	20 °C	95 °C	Open cell voltage (V)	Maximum power density (mW/cm^2)	Current density at 0.6 V (mS/cm^2)	Open cell voltage (V)	Maximum power density (mW/cm^2)	Current density at 0.6 V (mS/cm^2)
Recast Nafion®	25.8	53.3	0.97	713	1018	0.98	417	619
NM/GO-0.05	36.7	72.4	0.98	886	1376	0.94	586	826
NM/GO-0.10	40.8	82.3	0.98	743	1059	0.95	450	595
NM/GO-0.15	22.3	47.5	0.96	836	1215	0.95	509	652
Nafion® 212	40.8	88.3	0.99	951	1347	0.98	563	740

Table 4 Electrochemical properties exhibited by HPGFs and Pt/C catalyst at different physical parameters.

Catalysts	Surface area (m^2/g)	N content (%)	Pyridinic N (%)	Graphtic N (%)	Oxidized N (%)	Onset potential (V)		Limiting current density (mA/cm^2)	
						KOH	$HClO_4$	KOH	$HClO_4$
HPGF-1	918.7	3.15	37.9	51.9	10.2	1.03	0.81	9.08	9.90
HPGF-2	325.9	5.49	41.9	52.0	6.1	0.99	0.81	5.87	5.05
HPGF-3	567.7	3.09	36.8	50.6	12.6	0.97	0.80	7.33	5.27
Pt/C (20 wt%)	–	–	–	–	–	1.04	1.00	5.51	5.40

Reproduced with permission from Ref. [40], Copyright 2016, Elsevier

electrode (Fig. 12). The doped nanocomposite material showed the power density of 1008 mW/cm^2 at a current density of 6300 mA/m^2. This is a good metal free nanocomposite material which showed better performance in MFC.

2.3 Carbon Nanotubes and Its Hybrid Nanocomposites

Carbon nanotubes (CNT) are an important class of materials which significantly used in the field of material science, nanotechnology, optics, electronics, sensors, energy materials [42] due to their excellent mechanical, electrical and optical properties. Due to their light weight and high electrical conductivity, both Single-Walled Carbon Nanotubes (SWCNT) and Multi-Walled Carbon Nanotubes (MWCNT) [43] have obtained substantial consideration in FC application. They tend to increase the catalytic performance, steadiness, corrosion resistance, electron

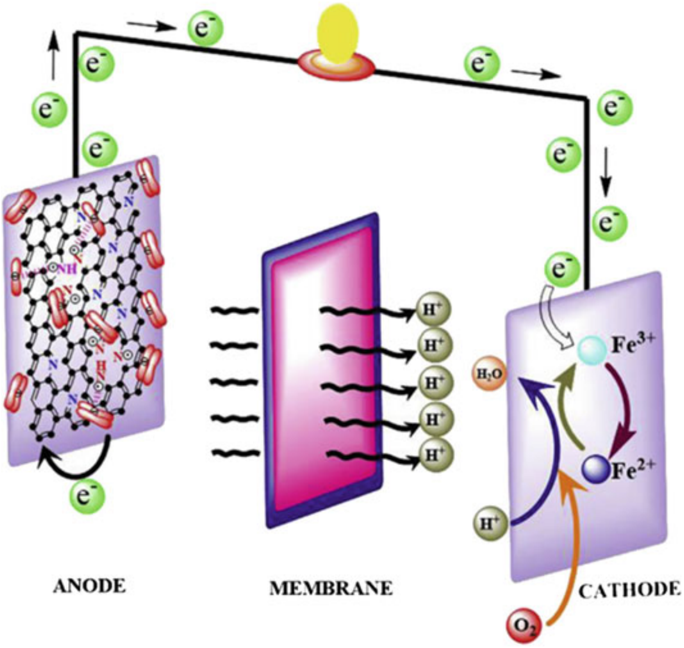

Fig. 12 Predicted mechanism involved in the electrogenic bacterial attachment to NGNS/cathode catalyst. Reproduced with permission from Ref. [41], Copyright 2015, Elsevier

transmission capacity and decreases the overall fuel cell cost [44]. Therefore, their usage as nanocomposite materials has extensively been studied in FC applications, especially in MFC.

CNT as an alternative cathode support and catalyst in MFCs was demonstrated by preparing a hybrid material containing CNT/Pt enriched with Palm Oil Mill Effluent. This material showed a better catalytic activity than undecorated Pt metal [45]. Incorporation of only 25% of Pt in the hybrid material reduced the use of precious Pt metal and thus helped in reducing the cost of FC. The material increased the MFC output voltage from 31.8 to 169.7 mW/m^2 at the chemical oxygen demand of 100 mg/L and 2000 mg/L, respectively which becomes a novel material as a catalyst in FC.

In 2014, Mehdinia et al. [46] compared the electrochemical performance of MFC using MWCNT-SnO_2/Glassy Carbon Electrode (GCE), MWCNT/GCE and bare GCE as anode material. From this experiment, it was concluded that the fabricated MWCNT-SnO_2/GCE (Fig. 13) produced a high electrochemical activity owing to the insertion of SnO_2 and high electron conductivity, high surface area properties of MWCNT into GCE. The power densities of MWCNT-SnO_2/(GCE), MWCNT/GCE, and bare GCE anode were found to be 1421, 699, 457 mW/m^2 respectively. Finally, the MWCNT-SnO_2/(GCE) nanocomposite represented as the best anode material for MFC due to its clean and green preparation and high electrochemical activity.

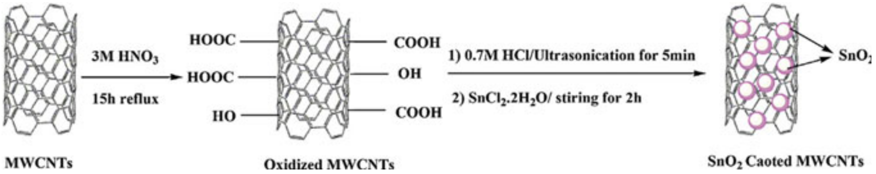

Fig. 13 Schematic representation of the synthesis of MWCNT/SnO_2 nanocomposite as an electrode material. Reproduced with permission from Ref. [46], Copyright 2014, Elsevier

A new MWCNT nanocomposite membrane modified with imidazole groups (MWCNT-Im) on Nafion® as proton conducting units showed the less methanol permeability, fuel crossover, and high proton conductivity in DMFC [47]. The combined interfacial attraction between the MWCNT grafted with protonated imidazole units, and a negatively charged sulfonic acid group of the Nafion® fluoropolymer formed a new electrostatic interaction. IEC was observed to be increased from 0.89 meq/g of Nafion® 117–0.92 meq/g of MWCNT-Im due to the participation of imidazole functional groups as new proton conduction sites added to the proton conduction mechanism. In addition, Nafion® modified with 0.5 wt% MWCNT-Im exhibited decreased methanol permeability of 1×10^{-6} cm^2/s with increasing in temperature by holding methanol molecules through a formation of complex structure. Overall, compared to neat Nafion®, the modified nanocomposite material showed excellent performance and accepted as a promising material in the application of FC.

In other work, a versatile metal-free catalyst for oxygen reduction reaction in FC was designed by Zhong et al. [48] They reformed the nitrogen, iron, and cobalt functionalized CNT (FeCoN-CNTs) with N-doped carbon foams (NCFs) with a 3D structure which provides a strong porous structure and large catalytically active sites. The composite material exhibited a synergetic effect of Fe/Co and the N species by forming the Fe/Co–N_x complex in the carbon material. In comparison with the commercial Pt/C catalyst, the newly fabricated material showed better performance in terms of resistance for fuel crossover and electrocatalysis in alkaline medium.

Recently, MWCNT functionalized with manganese oxide/polypyrrole (MWCNT-MnO_2/PPy) as an anode material in MFC was successfully demonstrated to produce the electricity from sewage water [49]. They electrochemically deposited the MWCNT-MnO_2/PPy on the surface of carbon cloth electrode as shown in Fig. 14. The fabricated electrode displayed electrical conductivity of 0.1185 S/m along with the band gap value of 0.8 eV and power density of 112.5.4 mW/m^2. Hence, it is a good example of MWCNT nanocomposite materials for generating the electricity from sewage source.

Mirzaei et al. [50] investigated a new catalyst support that made up of Pt/ MWCNT nanocomposite for PEMFC. This hydrothermally prepared catalyst support material achieved more activity even after 4000 cycles, whereas the Pt/C catalyst showed no activity after 2000 cycles. The nanocomposite material revealed

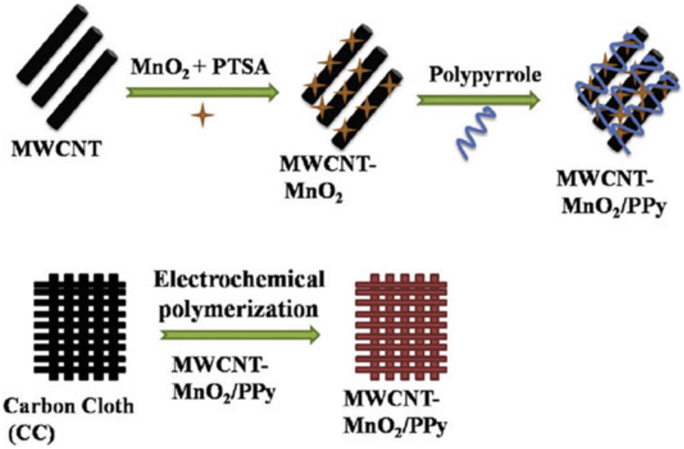

Fig. 14 Schematic representation of the synthesis of MWCNT-MnO_2/Ppy and proposed electrochemical polymerization on CC. Reproduced with permission from Ref. [49], Copyright 2016, Elsevier

Table 5 Comparison of the electrochemical and physical characteristics of Pt/MWCNTs and Pt/C.

Catalyst	Q_H (μc)	Specific surface area (m^2/g)	Particle size (nm)	Specific surface area (m^2/g) after 4000 cycle	OCV (V)
Pt/MWCNTs	0.178	36.46	7	5.37	+0.9
Pt/C	0.700	52.08	3.9	0.58	+0.96

Reproduced with permission from Ref. [50], Copyright 2017, Elsevier

Electrochemical Specific Surface Areas (ECSA) were initially 52.08 m^2/g was reduced to 0.58 m^2/g after 4000 cycles. Also showed good catalyst stability by achieving the ECSA value from 36.46 to 5.37 m^2/g (Table 5).

The HNO_3–H_2SO_4 functionalized CNT nanocomposite with MnO_2 demonstrated good catalyst for ORR in MFC maintained in neutral solution [51]. The ORR was increased by the unique interaction between MnO_2 and CNT which was fabricated through hydrothermal method. From the electrochemical measurements, it was observed that the MFC incorporated with the present material reached a power density of 520 mW/m^2 which is higher than the pristine CNT (275 mW/m^2) and MnO_2 with HNO_3–H_2SO_4 functionalized CNT (fCNT) (440 mW/m^2). Furthermore, the columbic efficiency was found to be 28.65% which was higher than the three mentioned material. Finally, it was concluded that the material is an excellent replacement for Pt/C catalyst material in MFC.

2.4 Chitosan-Based Nanocomposites

Chitosan is an environmental friendly biopolymer (polysaccharide), and hence was employed in significant applications including in the fields of biology, agriculture, industries, pharmaceutical, drug delivery system, dye removal and energy materials [52–57] due to its high molecular weight, antifungal activity, biocompatibility, gelation property, well-controlled structure and conduction capability. The usage of chitosan in FC development has received much attention in recent years owing to its extraordinary properties like that low cost, eco-friendly, hydrophilicity, low methanol permeability and ease of modifications of the polymer backbone of chitosan with other materials [58]. Chitosan can be used as an electrode and polymer electrolyte membrane in FC.

Bai et al. [59] designed a halloysite nanotube which is containing polyelectrolyte brushes (SHNTs) and it was incorporated into chitosan membrane. SHNTs generated a strong electrostatic interaction with the chitosan chain which improved the thermal and chemical properties by inhibiting the chain mobility. The nanocomposite membrane also overcome the problem of proton conduction in DMFC in an effective way by showing the highest conductivity of 18.6 mS/cm and IEC value of 0.204 mmol/g (Fig. 15) with an increase in the concentration of SHNT.

The phosphate and triphosphate salt complex membranes were inserted into chitosan membrane using chitosan hydrogel as electrode binder for increasing the proton conducting property in borohydride FCs [60]. This modified membrane was reached the highest power density of 685 mW/cm^2 at 60 °C which is almost 50% higher than the commercial Nafion® membrane. Also, the modified nanocomposite membrane showed a highest thermal stability of 200 °C as shown in Fig. 16.

A triple layer chitosan nanocomposite membrane having high efficiency in terms of power output, methanol permeability and proton exchange were demonstrated by Sadrabadi and group [61]. They coated two thin layers of chitosan on both the sides of Nafion® 105, chitosan acts as methanol barrier layer due to the presence of amino and hydroxyl group. Further, proton conductivity, methanol permeability, open circuit voltage measurements were proved too superior for multilayer Nafion®117 membranes with the thickness of 150–170 μm. In addition, power output was found to be 68.10 mW/cm^2 by feeding 5 M methanol which is 72% more than that of Nafion®117 membranes. Moreover, the lesser methanol crossover, ease of preparation and low cost will be the advantages to use as polyelectrolyte for DMFC (Table 6).

Chitosan was modified with polymeric reactive dyes which are containing quaternary ammonium groups (PRDQA) through blending followed by dyeing processes and studied for OH^- conduction in AFC [62]. The combined framework of CTS/PRDQA (1:0.5 by mass) nanocomposite membrane was exhibited an excellent OH^- conductivity of 8.17 mS/cm at room temperature (Table 7). The highest power density of 29.1 mW/cm^2 at a current density of 57.4 mA/cm^2 and open circuit voltage of 991.6 mV in an H_2/O_2 system was achieved which is appreciably better performance than pristine CTS membrane.

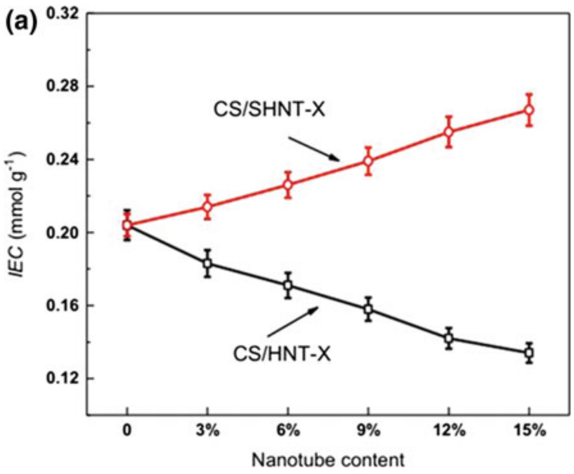

Fig. 15 A comparison of chitosan control and nanohybrid membranes at 25 °C at 100% RH in **a** IEC and **b** proton conductivity. Reproduced with permission from Ref. [59], Copyright 2014, Elsevier

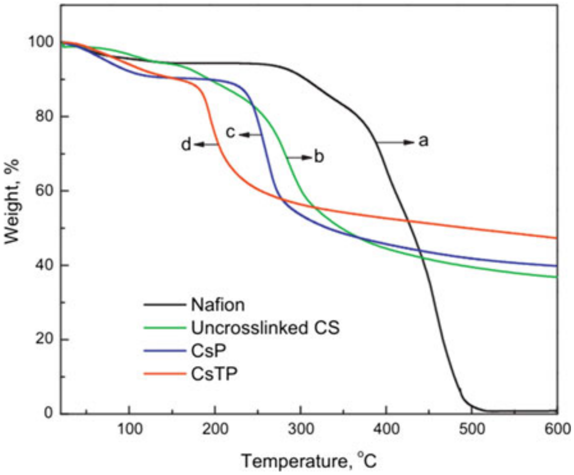

Fig. 16 TGA thermograms to demonstrate the stabilities of **a** Nafion®, **b** pristine chitosan, **c** chitosan modified with phosphate (CsP) and **d** chitosan modified with triphosphate (CsTP) membranes. Reproduced with permission from Ref. [60], Copyright 2012, Elsevier

Table 6 Methanol crossover current density at open circuit condition and limiting current density of various MEAs at 1 M and 5 M methanol concentrations at 70 °C

Sample	Methanol concentration (M)	Crossover current (mA/cm^2)	Limiting current (mA/cm^2)
Nafion®117	1.0	156	530
Nafion®117	5.0	518	260
CGS-12	1.0	142	445
CGS-12	5.0	460	285
Multi-layer	1.0	136	575
Multi-layer	5.0	420	385

Reproduced with permission from Ref. [61], Copyright 2012, Elsevier

Table 7 Physical and chemical properties of CTS/PRDQA membrane at room temperature

CTS/PRDQA (by mass)	WU (g/g)	Σ (× 10^{-3} S/cm)	Swelling ratio		IEC (meqiv./g)
			Δ S/S (%)	Δ V/V (%)	
1:0.125	0.82	2.15	41.65	81.17	0.41
1:0.25	0.73	3.92	33.93	73.89	0.65
1:05	0.67	8.17	24.44	65.42	1.08
1:0.75	0.62	9.09	21.52	49.69	1.24

Reproduced from Ref. [62], Copyright 2016, ESG

Li et al. [63] designed a matrix by incorporating a varying amount of chitosan nanoparticles into quaternized polyvinyl alcohol (QPVA) (Fig. 17) for FC applications. The modified matrix with 10% chitosan nanoparticle showed better suppression of methanol permeability and higher ionic conductivity than pristine QPVA. Also, they have prepared glutaraldehyde cross-linked nanocomposite film which has exhibited superior peak power density of 67 mW/cm^2 in DMFC.

Free-standing Chitosan/Phosphotungstic acid membranes for H_2O_2 FCs were reported recently [64]. To induce the chitosan crosslinking, the membrane was prepared by using anodic alumina as a porous medium to liberate the oxo-metallate anions as illustrated in Fig. 18. The peak power density of the membrane was found to be 350 mW/cm^2 and polyelectrolyte conductivity was 18 mS/cm which provided the excellent properties for the development of FC.

Pt-chitosan incorporated to $LaFeO_3$ nanoparticles with CNT has been studied for methanol electrooxidation in DMFC [65]. They prepared a layer by layer electrode material from modified Glassy Carbon (GC) with Pt nanoparticles (PtNPs), $LaFeO_3$NPs, CNT and chitosan as a binder. Integration of LaFeO3NPs and CNT material promoted the catalytic performance of the cell due to the presence of CNT decreased the dissolution of Pt. The method also reported that the methanol oxidation can be improved with the loading of a small amount of Pt.

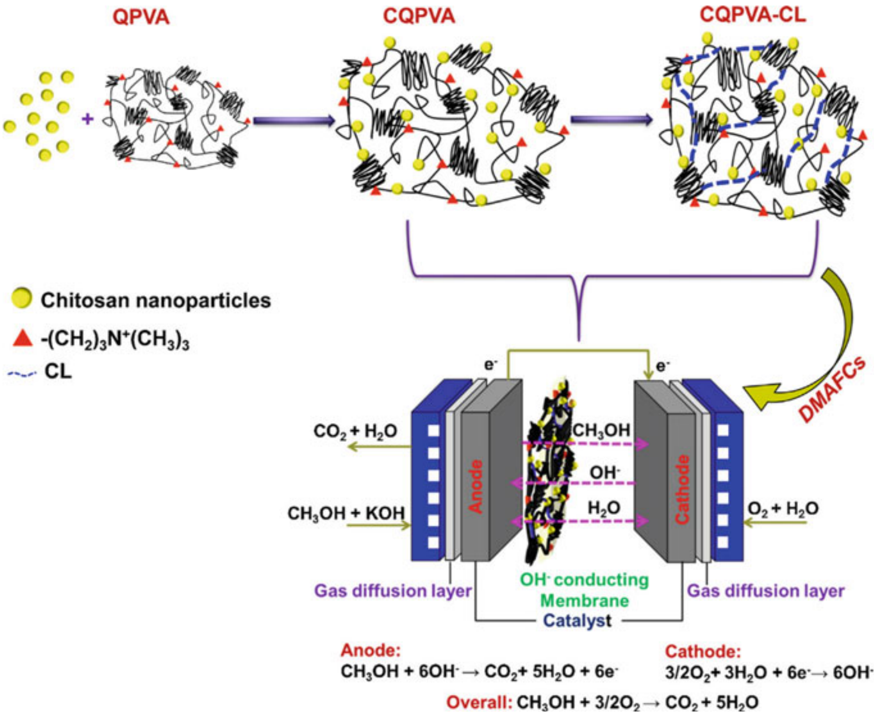

Fig. 17 Pictorial representation of glutaraldehyde cross-linked chitosan nanoparticle membrane for DMFC. Reproduced with permission from Ref. [63], Copyright 2016, Elsevier

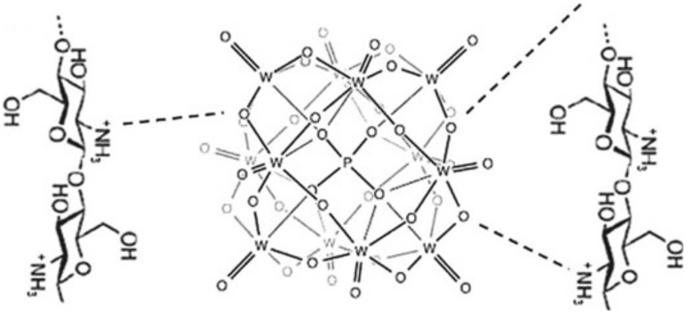

Fig. 18 Schematic representation of crosslinking the chitosan to the anionic species PTA^{3-}. Reproduced with permission from Ref. [64], Copyright 2015, Elsevier

2.5 Polybenzimidazole (PBI) Based Nanocomposite Membranes

PBI is a synthetic fiber and it has extraordinary properties such as high thermal stability, flame resistance capacity, moisture regains, retention of stiffness led to the development of high temperature operating devices. The close chain packing in PBI increases the hydrogen bonding and provides the rigidity to the materials. The use of PBI in FC has obtained utmost importance because of its high proton exchanging capacity, thermal and mechanical stabilities. PBI nanocomposite materials are excellent in proton conductivity when doped with acids like phosphoric acid because of its plasticizing property. In addition, the low gas permeability, zero water-electro osmotic drag, high CO poisoning tolerance has delivered the use of PBI units as nanocomposite membranes for high-temperature operating FCs.

Linlin et al. developed a composite material by incorporating silica in PBI to obtain high proton conductivity as well as to overcome the problem of acid leaching in acid doped PBI (dABPBI) based FCs [66]. They prepared poly (2,5-benzimidazole) (ABPBI) and embedded them on silica membrane in a methanesulfonic acid solvent to fabricate ABPBI-Si as described in Fig. 19. This modified sulfonated silica-ABPBI matrix improved the water uptake, mechanical and thermal stabilities. Similarly, the proton conductivity observed was 38 mS/cm at 140 °C and 1% RH which is a two-fold increase compared to the bare dABPBI membrane. Thus, it proved to be a promising nanocomposite membrane for FC at a higher temperature.

In a related work, Suryani and co-workers [67] incorporated silica on PBI membrane using N-(p-carboxyphenyl)maleimide (pCPM). This functionalized silica (SNP-pCPM) increased the interfacial compatibility between PBI and silica nanoparticles (SNPs) in PBI/SNP as described in Fig. 20 which created a proton conducting channel. This material was further used as nanofillers for the preparation

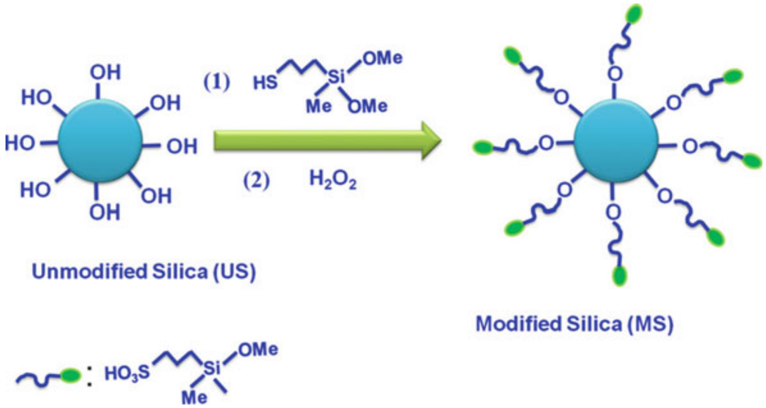

Fig. 19 Schematic representation of silica nanoparticles with methanesulfonic acid. Reproduced with permission from Ref. [66], Copyright 2012, Elsevier

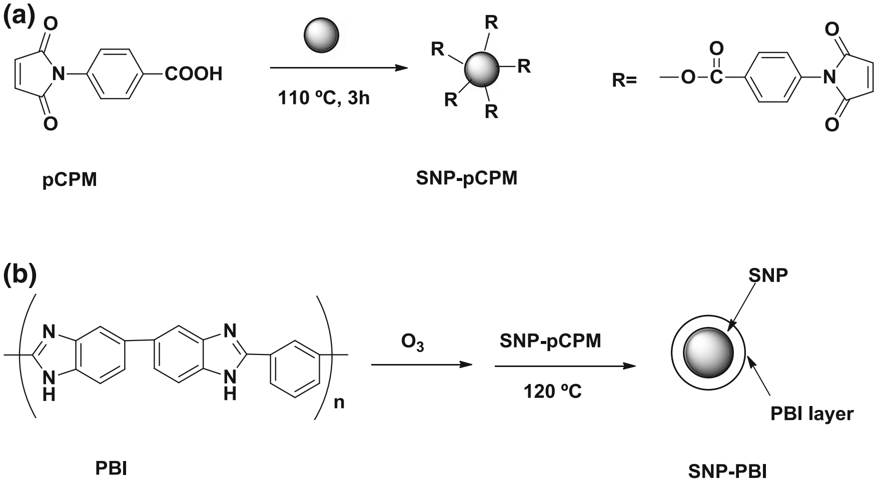

Fig. 20 **a** Functionalization of pCPM with silica nanoparticles **b** PBI functionalization with silica modified pCPM for proton conducting electrolyte membrane in FCs

of PBI/SNP-PBI membrane. With this modification, FCs displayed an excellent proton conductivity of 50 mS/cm at 160 °C by the use of 10 wt% composition of SNP-PBI. Also, a high power density of 650 mW/cm^2 was achieved in a single cell test which is higher than that of pristine PBI membrane.

The proton conductivity of PBI membrane was increased by functionalizing with Barium Zirconate ($BaZrO_3$) [68]. This modification increased the proton conduction to 125 mS/cm at 180 °C and 5% RH. At the same condition, the power density of 56 mW/cm^2 and a current density of 1120 mA/cm^2 were attained by the use of 4 wt% $BaZrO_3$ as nanofillers in PBI-$BaZrO_3$ (PBZ) membrane. This material proved to be a promising polyelectrolyte in FC membranes to improve proton conduction.

PBI/SiO_2 nanocomposite membranes were used to enhance the proton conduction membranes in PEMFC [69]. 5 wt% of SiO_2 as inorganic nanofiller was cast with PBI in dimethylacetamide solvent. The presence of SiO_2 facilitated proton conduction and acid retention properties. The nanohybrid membrane attained a conductivity of 102.7 mS/cm at 180 °C. Further, maximum cell voltage attained by this nanohybrid was found to be 0.6 V as 240 mA/cm^2.

A new material consisting of PBI functionalized with CNT was found to be very useful in FC applications. Wu et al. [70] doped this PBI/CNT and PBI membranes with KOH solution to make it more hydroxide conductive in ADMFC. They supplied the FC with 2 M methanol in 6 M KOH as anode fuel and humidified oxygen as oxidant at the cathode. This system attained a power density of 104.7 mW/cm^2 at 90 °C. In addition to this, thermal stability was enhanced and methanol permeability was reduced after the loading of 0.05–1% PBI functionalized CNT into PBI matrix. Therefore, it is considered to be a potential nanocomposite membrane for ADMFC.

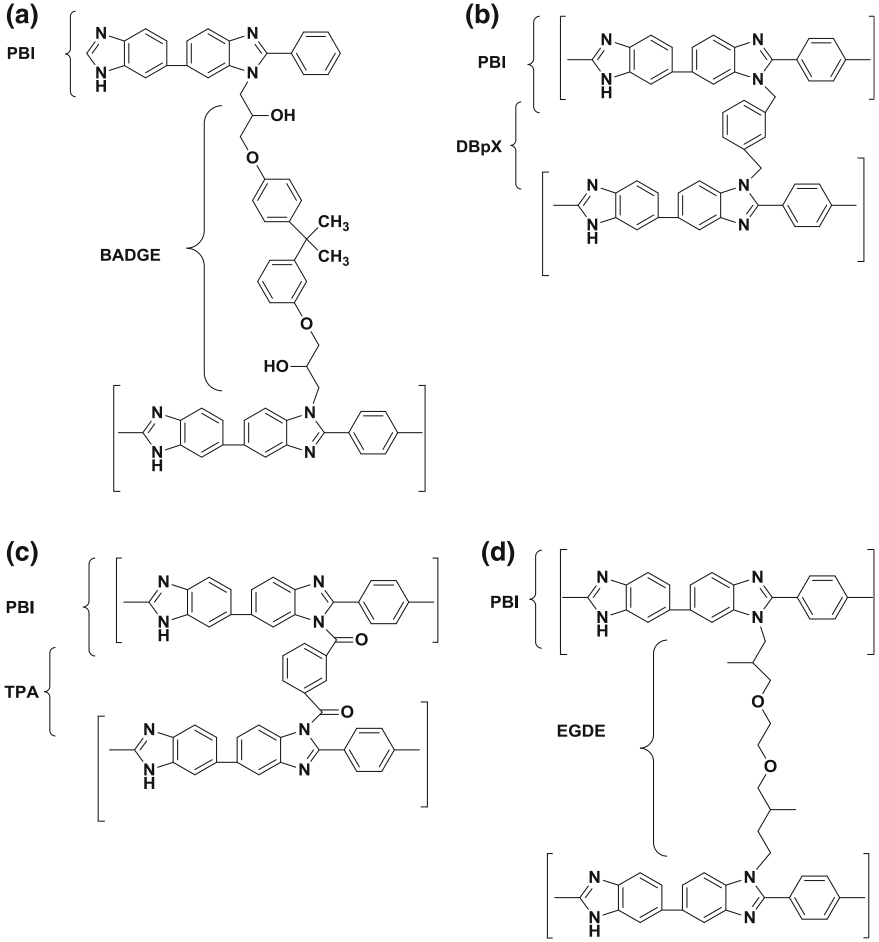

Fig. 21 Mechanism showing the crosslinking of **a** PBI/BADGE, **b** PBI/DBpX, **c** PBI/TPA and **d** PBI/EGDE. Reproduced with permission from Ref. [71], Copyright 2017 Elsevier

Recently, Özdemir et al. [71] studied the efficiency of PBI membranes fabricated with various cross-linkers for PEMFC. They cross-linked the PBI membrane with bisphenol A diglycidyl ether (BADGE), ethylene glycol diglycidyl ether (EGDE), α-α′-dibromo-p-xylene (DBpX) and terephthaldehyde (TPA) as illustrated in Fig. 21. From the electrochemical analysis, it was evident that PBI/BADGE nanocomposite membrane presented the superior acid retention property, however poor proton conduction. On the other hand, PBI/DBpX membrane was reached the maximum proton conductivity of 151 mS/cm at 180 °C. Meanwhile, PBI/BADGE composite materials exhibited maximum power density of 0.123 W. Therefore, they concluded that the PBI/BADGE and PBI/DBpX nanocomposite membranes are well suited for the polyelectrolyte membranes in FCs.

2.6 Poly (ether ether ketone) Based Nanocomposite

Poly (ether ether ketone) (PEEK) are the organic thermoplastics which have been used extensively for the modification of PEM in FC due to their high thermal and mechanical stabilities. High proton conductivity was noticed when they are cast in organic solvents as they permit the direct electrophilic sulfonation [72]. There are few reports on the preparation of sulfonated PEEK (SPEEK) membrane to increase the efficiency of PEM in FC [73]. However, there are some limitations like methanol crossover and less stability in FC caused by the high sulfonation in these membranes. Therefore, the modifications of SPEEK membranes require good maintenance and skills in preparation methods.

Modified PEM was prepared by incorporating SPEEK in poly (ether sulfone) (PES) in MFC at different concentration [74]. The conductivity of PES membranes was increased with 3–5% of SPEEK addition as summarized in Table 8. At 5% of SPEEK addition, the membrane achieved a high power density of 17,000 mW/cm^2. Further, the conductivity was reduced from 0.000615 to 0.0693 mS/cm and capacitance was reduced from 3.0×10^{-7} to 1.56×10^{-3} F. Such performance of nanocomposite materials are due to the sulfonated groups present which enhance the hydrophilic nature of the SPEEK membrane. Eventually, the modified PES membranes were considered as the best replacing PEM material to Nafion® 112 and 117 for MFC applications.

Later in 2013, the functionalization of SPEEK membranes with organically functionalized GO (SSi-GO) for DMFC applications was reported [75]. The synthesized material made up of SPEEK and sulfonated GO with further oxidation was carried out as shown in Fig. 22.

Integration of this material into the membrane increased the proton conductivity and lower the methanol permeability when compared to pristine Nafion® 112 and Nafion® 115 membranes (Table 9). Similarly, the condensed matrix of SSi-GO membrane established high mechanical and chemical stabilities.

The incorporation of sulfonated GO (s-GO) in SPEEK was investigated for the efficient FC functions [76]. The embedded SPEEK/s-GO composite membrane

Table 8 The modified nanocomposites with high performance to increase the efficiency of MFC

Type of membrane	Max. power density (mW/m)	Current density (mA m^{-2})	COD removal (%)	E_c (%)
N-112	0.003	0.124	55 ± 2	1.0 ± 0.4
N-117	3.630	9.842	60 ± 2	14.9 ± 5.5
PES	0.030	0.011	64 ± 4	0.5 ± 0.2
PES/SPEEK 3%	0.065	0.181	66 ± 6	5.4 ± 1.4
PES/SPEEK 5%	6.665	17.527	68 ± 6	26.3 ± 13.3

Reproduced with permission from Ref. [74] Copyright 2012 Elsevier

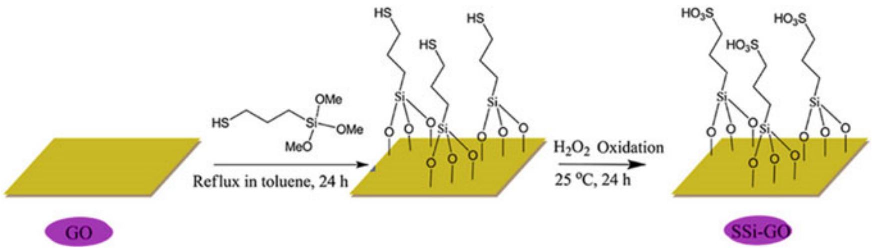

Fig. 22 Schematic illustration for the synthetic route of SSi-GO membrane. Reproduced with permission from Ref. [75], Copyright 2013, Elsevier

Table 9 Comparison of the efficiency of SPEEK membrane and modified SPEEK membranes [75]

Membrane	IEC (meq/g)	WU (%)	SW (%)	σ (mS/cm)	P ($\times 10^6$ cm^2/s)
SPEEK	1.710	40.1	15.5	88.1	1.15
SPEEK/GO (5 wt%)	1.704	33.1	13.8	98.3	0.59
SPEEK/SSi-GO (3 wt%)	1.792	38.5	16.2	146.7	0.72
SPEEK/SSi-GO (5 wt%)	1.864	49.9	17.0	160.2	0.83
SPEEK/SSi-GO (8 wt%)	1.872	50.9	18.3	162.6	1.36
Nafion® 112	0.941	37.1	13.9	125.4	1.53

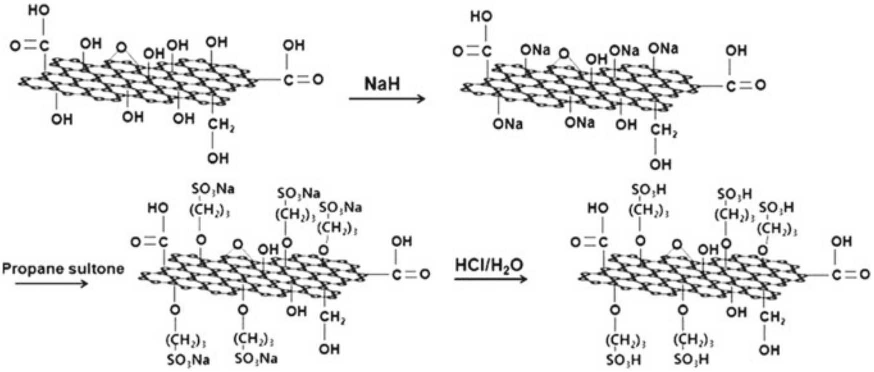

Fig. 23 A synthetic pathway for the sulfonation of GO to improve proton conduction. Reproduced with permission from Ref. [76], Copyright 2013, Elsevier

exhibited the improved proton conductivity of 8.41 mS/cm owing to the presence of high amount of sulfonic acid groups on the membrane (Fig. 23). The increased mechanical property of the membrane was attributed to the presence of strong hydrogen bonds between the s-GO and SPEEK. With the increase of GO content in the membrane, the elastic modulus and intrinsic strength were also increased. Thus, lower methanol permeability of 2.6388×10^{-7} cm^2/s was attained and therefore, it is considered to be the best nanocomposite material for the applications in DMFC.

Wang et al. prepared a novel anhydrous membrane for PEM by embedding the dopamine-modified silica nanoparticles ($DSiO_2$) into SPEEK polymer [77]. The enhancement of thermal and mechanical stabilities are due to uniformly dispersed $DSiO_2$ in SPEEK which is increased interfacial electrostatic attraction. There was an occurrence of high proton conduction at the acid-base site of SPEEK/$DSiO_2$ via Grotthuss mechanism due to the formation of small aggregation of sulfonic acid ionic channels. By the experimentation, it was revealed that the prepared hybrid membrane with 15% $DSiO_2$ achieved a conductivity of 4.52 mS/cm at 120 °C under anhydrous conditions. The membrane also attained a power density of 111.7 mW/cm^2 and open cell potential of 0.98 V which is considered to be the superior performance in PEM under anhydrous conditions.

Incorporation of novel nanomaterial as graphitic carbon nitride (g-C_3N_4) sheets into SPEEK membrane illustrated in Fig. 24 offers the superior efficiency compared to the pristine SPEEK membrane [78]. The fabricated SPEEK membrane with 5 wt % of g-C_3N_4, proton conductivity up to 786 mS/cm at 20 °C was achieved. As previously mentioned, the Grotthuss effect played a major role in the proton conduction due to the presence of acid-base pair at the composite site. Further, it favoured the resistance of methanol crossover and maintained the power density up to 39% due to the periodic vacancies in the lattice of the g-C_3N_4 membrane. Therefore, this is accepted to be the best nanocomposite materials for FC applications.

Sulfated zirconia nanoparticles with SPEEK modified nanocomposites (Fig. 25) were found to be the best composite materials for FCs [79]. The combination of

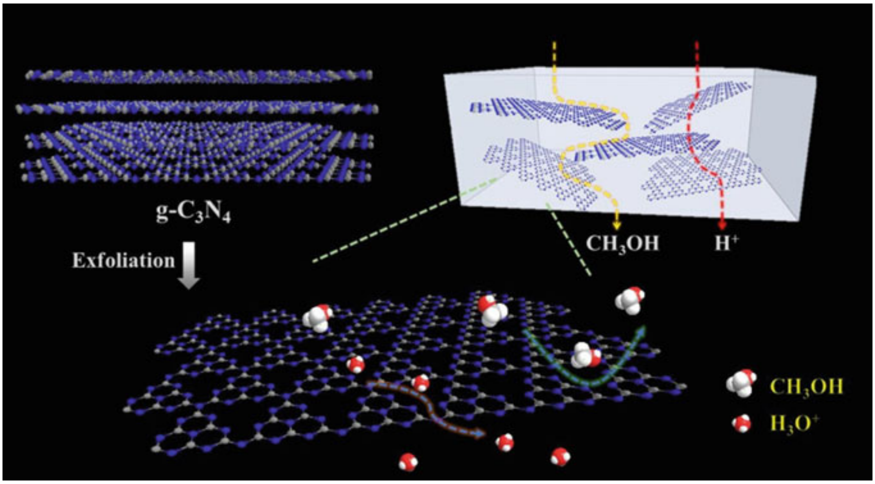

Fig. 24 Schematic illustration of the incorporation of g-C_3N_4 into SPEEK nanocomposite membrane. Reproduced with permission from Ref. [78], Copyright 2016, Elsevier

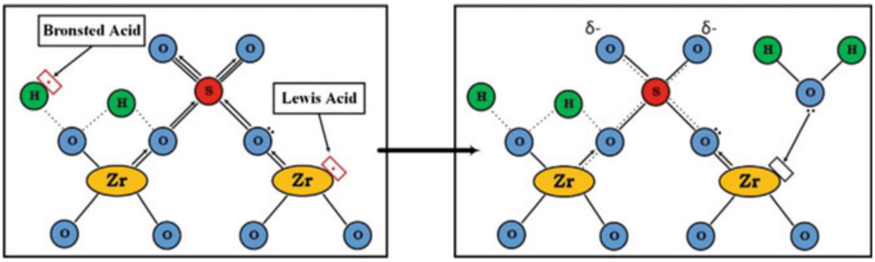

Fig. 25 Representation of the surface modification of SPEEK with sulfated zirconia nanoparticles. Reproduced with permission from Ref. [79], Copyright 2016, Elsevier

sulfonation time (6.9 h) and inorganic additives (5.94 wt%) produced the superior membranes. The proton conductivity observed was 3.88 mS/cm and oxidative stability of 102 min. In addition, the membrane also obtained the mechanical strength of 898 MPa.

SPEEK as an electrode ionomer material showed good catalytic activity for PEMFC [80]. The electrodes were prepared with 15, 25, 35 wt% of SPEEK and Pt content of 0.3, 0.4 and 0.5 mg/cm^2 were investigated for electrochemical reactions. The experiments demonstrated that the 25% of ionomer with 0.5 mg/cm^2 was found to be suitable for cathode catalyst for PEMFC.

2.7 Polyvinyl Alcohol (PVA) Based Nanocomposites

PVA is a water-soluble polymer with long chain 1, 3-diol linkages in its backbone. It has excellent film forming and emulsifying properties and hence is extensively used in membrane technology, adhesive materials development, and drug delivery etc. The flexibility, mechanical strength, thermal stability of PVA materials depends on the nature of cross-linkers used for material preparation. The excellent proton conduction capacity of organically modified PVA material attained importance in the development of nanocomposite materials in FC material applications.

The PVA modified with various poly(sulfonic acid) grafted silica nanoparticles were studied by Salarizadeh and co-workers [81]. First, they altered the surface of nanoparticles by APTES followed by preparing a nanocomposite membrane by various concentration from 0 to 20% of SNP with poly (styrene sulfonic acid) (PSSA-G-SNP), poly (2-acrylamido-2methyl-1-propane sulfonic acid) (PAMPS-g-SN) by using glutardialdehyde as a cross-linking agent as demonstrated in Fig. 26. It was observed that the membranes consisting of 5 wt% of PAMPS-g-SNP exhibited the better performance for FCs applications. This material showed the proton conductivity of 10.4 mS/cm by signifying that sulfonation of silica nanoparticles by grafting of sulfonated polyelectrolyte which increased the proton conductivity. Meanwhile, the

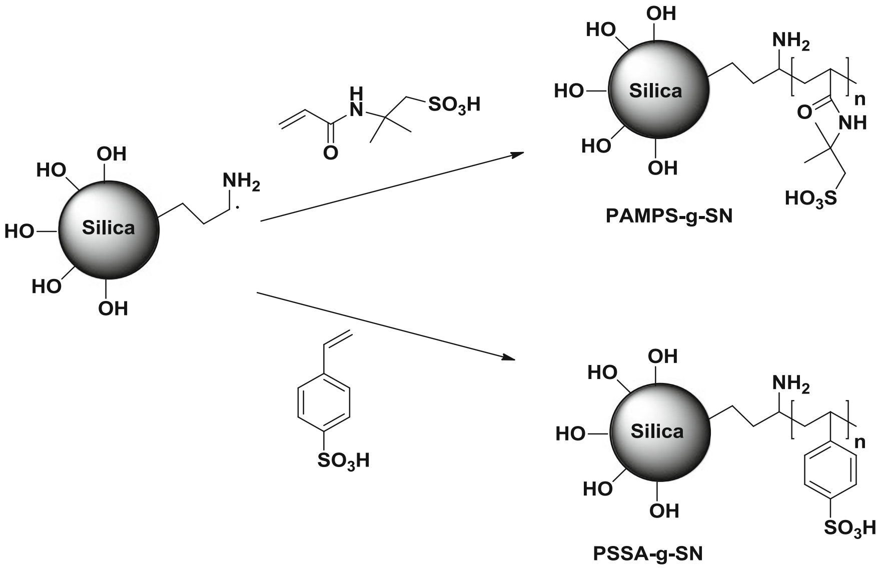

Fig. 26 Mechanism of surface-initiated free radical polymerization of AMPS and SSA onto APTES modified silica nanoparticles initiated by Ce(IV)-based redox initiation system. Reproduced with permission from Ref. [81], Copyright 2013, Elsevier

water uptake capacity was also increased for the same concentration, then diminished rapidly. Therefore, it was concluded that the prepared membrane can be effectively used for high proton conduction in FC.

A new variety of PEM for FCs prepared by PVA and the ionic liquid was reported by Liew et al. [82]. The prepared nanocomposite membrane with PVA/ammonium acetate/1-butyl-3-methylimidazolium chloride (BmImCl) reveals that increased ionic conductivity with ionic liquid mass loading. After the addition of 50 wt% of BmImCl, the PEM reached the highest ionic conductivity 5.74 ± 0.01 mS/cm. This was due to the fact that the addition of ionic liquid enhanced the plasticizing effect to the membrane. In addition, the nanocomposites also exhibited the thermal stability of up to 250 °C and achieved a maximum power density of 18 mW/cm^2 at room temperature with an operational current of 750 mA.

In 2014, a nanocomposite membrane was prepared by cross-linking of PVA with aryl sulfonated graphene oxide (SGO) for versatile applications in FC material [83]. The modification of the GO surface with aryl diazonium salt of the sulfanilic acid by further introducing 5 wt% SGO into PVA matrix by using glutaraldehyde as a cross-linking agent. The hybrid membrane showed high thermal stability with melting temperature of 223 °C, the tensile strength of 67.8 MPa and proton conductivity of 50 mS/cm. The increased proton conductivity owing to the interaction between—SO_3H of SGO and –OH group of GO via Grotthuss mechanism and Vehicle mechanism was explained in Fig. 27. Furthermore, the power density of 16.15 mW/cm^2 was attained. Overall, the modified PVA/SGO nanocomposite

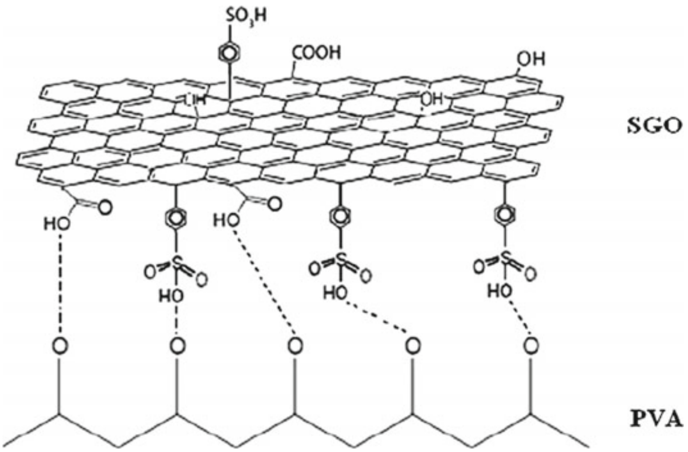

Fig. 27 Schematic representation of the reaction between PVA and SGO nanoparticles. Reproduced with permission from Copyright 2014, [83], American Chemical Society

membrane showed higher efficiency compared to unmodified GO and Nafion® membranes in terms of thermal stability and proton conductivity.

In other work, a novel hybrid membrane based on the infiltration of a blend of SPEEK with PVA in water and SPEEK blended with polyvinyl butyral (PVB) into electrospun nanofibres were reported [84]. A covering of hydrated SPEEK-30% PVB showed better proton conductivity. Further, the nanofibre incorporation into SPEEK-PVA matrix improved the mechanical stability, and methanol barrier capacity as explained in Table 10. Eventually, the prepared membrane was found useful for the applications in DMFC.

Yang et al. [85] prepared a blended membrane consisting of PVA and sodium alginate (PVASA) polymers of various concentration for alkaline solid PEM. This was further treated with glutaraldehyde to form a cross-linked membrane of PVASA (PVASA-GA). From the electrochemical measurements, it was observed that the ionic conductivity was found to be 91 mS/cm at 25 °C for the membrane containing 60:40 of PVA and SA. In addition, the methanol permeability was achieved in the order of 10^{-7} cm^2/s. On the other hand, the membrane prepared with 80:20 of PVA and SA cross-linked with GA up to 60 min, exhibited the selectivity value of 21.50×10^3 S/cm^3s^1. Also, the PVASA with 80:20 composition showed a maximum power density of 20.7 mW/cm^2 which was achieved at $E_{p.max}$ with a peak current density of 89.20 mA/cm^2 at 30 °C. Therefore, the membrane was found to be extensively used in DMFC application.

Recently, the application of PVA modified with functionalized CNT (m-CNT) in ADEFC was reported [86]. Addition of m-CNT into PVA membrane increased the alkaline uptake and ionic conductivity of KOH doped electrolyte membrane. At the same time, a lower swelling ratio and ethanol permeability were suppressed in comparison with pristine PVA membrane. Also, the highest power density of 65 mW/cm^2 at 60 °C was achieved.

Table 10 Comparison of the performance of nanocomposite and SPEEK-35% PVA

Membrane	Crosslinking temperature (°C)	Metahnol permeability(cm^2/s)	Proton conductivity(S/cm)	Modified characteristic factor (S^2 s cm^{-4})
SPEEK-35% PVA	110	$5.81 \pm 0.20 \times 10^{-6}$	$1.11 \pm 0.08)\cdot 10^{-2}$	21.2 ± 3.2
Nanocomposite	110	$4.43 \pm 0.21 \times 10^{-6}$	$1.35 \pm 0.11)\cdot 10^{-2}$	41.1 ± 5.8
SPEEK-35% PVA	120	$4.70 \pm 0.13 \times 10^{-6}$	$1.10 \pm 0.05)\cdot 10^{-2}$	25.7 ± 1.9
Nanocomposite	120	$3.82 \pm 0.18 \times 10^{-6}$	$1.03 \pm 0.08)\cdot 10^{-2}$	27.8 ± 3.6
SPEEK-35% PVA	130	$2.18 \pm 0.07 \times 10^{-6}$	$5.84 \pm 0.32)\cdot 10^{-3}$	15.6 ± 1.5
Nanocomposite	130	$2.02 \pm 0.11 \times 10^{-6}$	$2.50 \pm 0.18)\cdot 10^{-3}$	3.1 ± 0.3
SPEEK-35% PVA	140	$1.19 \pm 0.06 \times 10^{-6}$	$3.53 \pm 0.13)\cdot 10^{-3}$	10.5 ± 0.3
Nanocomposite	140	$1.34 \pm 0.09 \times 10^{-6}$	$1.63 \pm 0.10)\cdot 10^{-3}$	2.0 ± 0.1
Nafion® 115	_	$3.71 \pm 0.05 \times 10^{-6}$	$3.64 \pm 0.11)\cdot 10^{-2}$	357 ± 24

Reproduced with permission from Ref. [84], Copyright 2015, Elsevier

3 Conclusion

In this chapter, we summarized the current scenario of FC research and development around the world. The modification of composites with various nanomaterials is the developing technology to overcome the problems such as fuel crossover, low proton conduction, expensive raw materials, higher cost, and low membrane stability. The advantages of hybrid nanocomposites such as Nafion®, CNT, GO, SPEEK, PBI, PVA in FCs are comprehensively discussed. A variety of improved materials as anode, cathode, and membranes are elucidated. The improved efficiency of FCs in terms of high proton conduction, better water retention, suppression of fuel crossover, high chemical and thermal stabilities are precisely explained.

Acknowledgements The authors acknowledge the financial support from DST Nanomission, India (SR/NM/NS-20/2014), DST, India (DST-TM-WTI-2K14-213) and SERB-DST, India (YSS/2015/000013) for financial support. We also thank Jain University, India for providing facilities.

References

1. Hajilary N, Shahi A, Rezakazemi M (2018) Evaluation of socio-economic factors on CO_2 emissions in Iran: factorial design and multivariable methods. J Clean Prod 189:108–115
2. Hashemi F, Rowshanzamir S, Rezakazemi M (2012) CFD simulation of PEM fuel cell performance: effect of straight and serpentine flow fields. Math Comput Model 55(3–4):1540–1557
3. Winter M, Brodd RJ (2004) What are batteries, fuel cells, and supercapacitors? Chem Rev 104:4245–4269
4. Lemons RA (1990) Fuel cells for transportation. J Power Sources 29(1–2):251–264
5. Peighambardoust S, Rowshanzamir S, Amjadi M (2010) Review of the proton exchange membranes for fuel cell applications. Int J Hydrogen Energy 35(17):9349–9384
6. Giorgi L, Leccese F (2013) Fuel cells: technologies and applications. Open Fuel Cells J 6: 1–20
7. Agmon N (1995) The grotthuss mechanism. Chem Phys Lett 244(5):456–462
8. Ueki T, Watanabe M (2008) Macromolecules in ionic liquids: progress, challenges, and opportunities. Macromolecules 41(11):3739–3749
9. Rezakazemi M, Amooghin AE, Montazer Rashmati MM, Ismail AF, Matsuura T (2014) State-of-the-art membrane based CO_2 separation using mixed matrix membranes (MMMs): an overview on current status and future directions. Prog Polym Sci 39(5):817–861
10. Rezakazemi M, Razavi S, Mohammadi T, Nazari GA (2011) Simulation and determination of optimum conditions of pervaporative dehydration of isopropanol process using synthesized PVA–APTEOS/TEOS nanocomposite membranes by means of expert systems. J Membr Sci 379(1–2):224–232
11. Dashti A, Harami HR, Rezakazemi M (2018) Accurate prediction of solubility of gases within H_2-selective nanocomposite membranes using committee machine intelligent system. Int J Hydrogen Energy 43(13):6614–6624
12. Rezakazemi M, Vatani A, Mohammadi T (2016) Synthesis and gas transport properties of crosslinked poly(dimethylsiloxane) nanocomposite membranes using octatrimethylsiloxy POSS nanoparticles. J Nat Gas Sci Eng 30:10–18
13. Rezakazemi M, Vatani A, Mohammadi T (2015) Synergistic interactions between POSS and fumed silica and their effect on the properties of crosslinked PDMS nanocomposite membranes. RSC Adv 5(100):82460–82470
14. Rezakazemi M, Sadrzadeh M, Mohammadi T, Matsuura T (2017) Methods for the preparation of organic–inorganic nanocomposite polymer electrolyte membranes for fuel cells. In: Inamuddin D, Mohammad A, Asiri AM (eds) Organic-inorganic composite polymer electrolyte membranes. Springer International Publishing, Cham, pp 311–325
15. Sodeifian G, Mojtaba R, Asghari M, Rezakzemi M (2018) Polyurethane-SAPO-34 mixed matrix membrane for CO_2/CH_4 and CO_2/N_2 separation. Chin J Chem Eng. https://doi.org/10.1016/j.cjche.2018.03.012
16. Rezakazemi M, Dashti A, Asghari M, Saeed S (2017) H_2-selective mixed matrix membranes modeling using ANFIS, PSO-ANFIS GA-ANFIS. Int J Hydrogen Energy 42(22):15211–15225
17. Baheri B, Mahnaz S, Razakazemi M, Elahe M, Mohammadi T (2014) Performance of PVA/NaA mixed matrix membrane for removal of water from ethylene glycol solutions by pervaporation. Chem Eng Commun 202(3):316–321
18. Shahverdi M, Baheri B, Razakazemi M, Elahe M, Mohammadi T (2013) Pervaporation study of ethylene glycol dehydration through synthesized (PVA-4A)/polypropylene mixed matrix composite membranes. Polym Eng Sci 53(7):1487–1493
19. Rostamizadeh M, Rezakazemi M, Shahidi K, Mohammadi T (2013) Gas permeation through H_2-selective mixed matrix membranes: Experimental and neural network modeling. Int J Hydrogen Energy 38(2):1128–1135

20. Rezakazemi M, Mohammadi T (2013) Gas sorption in H_2-selective mixed matrix membranes: experimental and neural network modeling. Int J Hydrogen Energy 38(32):14035–14041
21. Rezakazemi M, Shahidi K, Mohammadi T (2012) Sorption properties of hydrogen-selective PDMS/zeolite 4A mixed matrix membrane. Int J Hydrogen Energy 37(22):17275–17284
22. Rezakazemi M, Shahidi K, Mohammadi T (2012) Hydrogen separation and purification using crosslinkable PDMS/zeolite a nanoparticles mixed matrix membranes. Int J Hydrogen Energy 37(19):14576–14589
23. Rezakazemi M, Sadrzadeh M, Matsuura T (2018) Thermally stable polymers for advanced high-performance gas separation membranes. Prog Energy Combust Sci 66:1–41
24. Boutsika LG, Enotiadis A, Nicotera I, Simari C, Charalambopoulou G, Giannelis EP, Steriotis T (2016) Nafion® nanocomposite membranes with enhanced properties at high temperature and low humidity environments. Int J Hydrogen Energy 41(47):22406–22414
25. Mohammadi G, Jahanshahi M, Rahimpour A (2013) Fabrication and evaluation of Nafion nanocomposite membrane based on ZrO_2–TiO_2 binary nanoparticles as fuel cell MEA. Int J Hydrogen Energy 38(22):9387–9394
26. Hooshyari K, Javanbhakt M, Naji L, Enhessari M (2014) Nanocomposite proton exchange membranes based on Nafion containing Fe_2 TiO_5 nanoparticles in water and alcohol environments for PEMFC. J Membr Sci 454:74–81
27. Wang Z, Tang H, Zhang H, Lei M, Chen R, Xiao P, Pan M (2012) Synthesis of Nafion/CeO_2 hybrid for chemically durable proton exchange membrane of fuel cell. J Membr Sci 421: 201–210
28. Cozzi D, de Bonis C, D'Epifanio A, Mecheri B, Tavares AC, Licoccia S (2014) Organically functionalized titanium oxide/Nafion composite proton exchange membranes for fuel cells applications. J Power Sources 248:1127–1132
29. de Bonis C, Cozzi D, Mecheri B, D'Epifanio A, Rainer A, De Porcellenis D, Licoccia S (2014) Effect of filler surface functionalization on the performance of Nafion/Titanium oxide composite membranes. Electrochim Acta 147:418–425
30. Yang Y, Cuiping H, Beibei J, James I, Chengen H, Dean S, Tao J, Zhiqun L (2016) Graphene-based materials with tailored nanostructures for energy conversion and storage. Mater Sci Eng R Rep 102:1–72
31. Farooqui U, Ahmad A, Hamid N (2018) Graphene oxide: a promising membrane material for fuel cells. Renew Sust Energy Rev 82:714–733
32. Tsang AC, Kwok HY, Leung DY (2017) The use of graphene based materials for fuel cell, photovoltaics, and supercapacitor electrode materials. Solid State Sci 67:A1–A14
33. Das TK, Prusty S (2013) Graphene-based polymer composites and their applications. Polym Plast Technol Eng 52(4):319–331
34. Zhu C, Dong S (2013) Recent progress in graphene-based nanomaterials as advanced electrocatalysts towards oxygen reduction reaction. Nanoscale 5(5):1753–1767
35. Fampiou I, Ramasubramaniam A (2012) Binding of Pt nanoclusters to point defects in graphene: adsorption, morphology, and electronic structure. J Phys Chem C 116(11): 6543–6555
36. Liu M, Zhang R, Chen W (2014) Graphene-supported nanoelectrocatalysts for fuel cells: synthesis, properties, and applications. Chem Rev 114(10):5117–5160
37. Huang H, Chen H, Sun D, Wang X (2012) Graphene nanoplate-Pt composite as a high performance electrocatalyst for direct methanol fuel cells. J Power Sources 204:46–52
38. Qian W, Hao R, Zhou J, Eastman M, Manhat BA, Sun Q, Andrea MG, Jiao J (2013) Exfoliated graphene-supported Pt and Pt-based alloys as electrocatalysts for direct methanol fuel cells. Carbon 52:595–604
39. Peng K-J, Lai J-Y, Liu Y-L (2016) Nanohybrids of graphene oxide chemically-bonded with Nafion: preparation and application for proton exchange membrane fuel cells. J Membr Sci 514:86–94
40. Zhou X, Tang S, Yin Y, Sun S, Qiao J (2016) Hierarchical porous N-doped graphene foams with superior oxygen reduction reactivity for polymer electrolyte membrane fuel cells. Appl Energy 175:459–467

41. Kirubaharan CJ, Santhakumar K, Gnanankumar G, Senthilkumar N, Jang J (2015) Nitrogen doped graphene sheets as metal free anode catalysts for the high performance microbial fuel cells. Int J Hydrogen Energy 40(38):13061–13070
42. Rezakazemi M, Zhang Z (2018) Desulfurization materials A2—Dincer, Ibrahim comprehensive energy systems. Elsevier, Oxford, pp 944–979
43. Georgakilas V, Perman JA, Tucek J, Zboril R (2015) Broad family of carbon nanoallotropes: classification, chemistry, and applications of fullerenes, carbon dots, nanotubes, graphene, nanodiamonds, and combined superstructures. Chem Rev 115(11):4744–4822
44. Akbari E, Buntat Z (2017) Benefits of using carbon nanotubes in fuel cells: a review. Int J Energ Res 41(1):92–102
45. Ghasemi M, Ismail M, Kamarudin SK, Saeedfar K, Wan Daud WR, Hassan SHA, Heng LY, Alam J, Oh SE (2013) Carbon nanotube as an alternative cathode support and catalyst for microbial fuel cells. Appl Energy 102:1050–1056
46. Mehdinia A, Ziaei E, Jabbari A (2014) Multi-walled carbon nanotube/SnO_2 nanocomposite: a novel anode material for microbial fuel cells. Electrochim Acta 130:512–518
47. Tohidian M, Ghaffarian SR (2017) Polyelectrolyte nanocomposite membranes with imidazole-functionalized multi-walled carbon nanotubes for use in fuel cell applications. J Macromol Sci B 56(10):725–738
48. Zhang R, He S, Lu Y, Chen W (2015) Fe Co, N-functionalized carbon nanotubes in situ grown on 3D porous N-doped carbon foams as a noble metal-free catalyst for oxygen reduction. J Mater Chem A 3(7):3559–3567
49. Mishra P, Jain R (2016) Electrochemical deposition of MWCNT-MnO_2/PPy nano-composite application for microbial fuel cells. Int J Hydrogen Energy 41(47):22394–22405
50. Mirzaei F, Parnian MJ, Rowshanzamir S (2017) Durability investigation and performance study of hydrothermal synthesized platinum-multi walled carbon nanotube nanocomposite catalyst for proton exchange membrane fuel cell. Energy 138:696–705
51. Liew KB, Wan Daud WR, Ghasemi M, Loh KS, Ismail M, Lim SS, Leong JX (2015) Manganese oxide/functionalised carbon nanotubes nanocomposite as catalyst for oxygen reduction reaction in microbial fuel cell. Int J Hydrogen Energy 40(35):11625–11632
52. Mourya V, Inamdar NN, Tiwari A (2010) Carboxymethyl chitosan and its applications. Adv Mater Lett 1(1):11–33
53. Vakili M, Rafatullah M, Salamatinia B, Abdullah AZ, Ibrahim MH, Tan KB, Gholami Z, Amouzgar P (2014) Application of chitosan and its derivatives as adsorbents for dye removal from water and wastewater: a review. Carbohyd Polym 113:115–130
54. Srinivasa P, Tharanathan R (2007) Chitin/chitosan—safe, ecofriendly packaging materials with multiple potential uses. Food Rev Int 23(1):53–72
55. Lim S-H, Hudson SM (2003) Review of Chitosan and its derivatives as antimicrobial agents and their uses as textile chemicals. J Macromol Sci C Polym Rev 43(2):223–269
56. Mourya V, Inamdar NN (2009) Trimethyl chitosan and its applications in drug delivery. J Mater Sci Mater Med 20(5):1057
57. Ilium L (1998) Chitosan and its use as a pharmaceutical excipient. Pharm Res 15(9): 1326–1331
58. Ma J, Sahai Y (2013) Chitosan biopolymer for fuel cell applications. Carbohydr Polym 92 (2):955–975
59. Bai H, Zhang H, He Y, Liu J, Zhang B, Wang J (2014) Enhanced proton conduction of chitosan membrane enabled by halloysite nanotubes bearing sulfonate polyelectrolyte brushes. J Membr Sci 454:220–232
60. Ma J, Sahai Y, Buchheit RG (2012) Evaluation of multivalent phosphate cross-linked chitosan biopolymer membrane for direct borohydride fuel cells. J Power Sources 202:18–27
61. Hasani-Sadrabadi MM, Dashtimoghadam E, Mokarram N, Majedi FS, Jacob KI (2012) Triple-layer proton exchange membranes based on chitosan biopolymer with reduced methanol crossover for high-performance direct methanol fuel cells application. Polymer 53 (13):2643–2651

62. Zhou T, He X, Song F, Xie K (2016) Chitosan modified by polymeric reactive dyes containing quanternary ammonium groups as a novel anion exchange membrane for alkaline fuel cells. Int J Electrochem Sci 11(1):590–608
63. Li P-C, Liao G-M, Rajeshkumar S, Shih C-M, Yang C-C, Wang D-M, Lue SJ (2016) Fabrication and characterization of chitosan nanoparticle-incorporated quaternized poly (vinyl alcohol) composite membranes as solid electrolytes for direct methanol alkaline fuel cells. Electrochim Acta 187:616–628
64. Santamaria M, Pecoraro CM, Di Quarto F, Bocchetta P (2015) Chitosan–phosphotungstic acid complex as membranes for low temperature H_2–O_2 fuel cell. J Power Sources 276: 189–194
65. Noroozifar M, Motlagh MK, Kakhki M-S, Roghayeh K-M (2014) Enhanced electrocatalytic properties of Pt–chitosan nanocomposite for direct methanol fuel cell by $LaFeO_3$ and carbon nanotube. J Power Sources 248:130–139
66. Linlin M, Mishra AK, Kim NH, Lee JH (2012) Poly (2,5-benzimidazole)–silica nanocomposite membranes for high temperature proton exchange membrane fuel cell. J Membr Sci 411:91–98
67. Chang Y-N, Lai J-Y, Liu Y-L (2012) Polybenzimidazole (PBI)-functionalized silica nanoparticles modified PBI nanocomposite membranes for proton exchange membranes fuel cells. J Membr Sci 403:1–7
68. Hooshyari K, Javanbhakt M, Shabanikia A, Enhessari M (2015) Fabrication $BaZrO_3$/PBI-based nanocomposite as a new proton conducting membrane for high temperature proton exchange membrane fuel cells. J Power Sources 276:62–72
69. Devrim Y, Devrim H, Eroglu I (2016) Polybenzimidazole/SiO_2 hybrid membranes for high temperature proton exchange membrane fuel cells. Int J Hydrogen Energy 41(23):10044–10052
70. Wu J-F, Lo C-F, Li H-Y, Chang C-M, Liao K-S, Hu C-C, Liu Y-L, Lue S-J (2014) Thermally stable polybenzimidazole/carbon nano-tube composites for alkaline direct methanol fuel cell applications. J Power Sources 246:39–48
71. Özdemir Y, Özkan N, Devrim Y (2017) Fabrication and characterization of cross-linked polybenzimidazole based membranes for high temperature PEM fuel cells. Electrochim Acta 245:1–13
72. Hogarth WH, Da Costa JD, Lu GM (2005) Solid acid membranes for high temperature proton exchange membrane fuel cells. J Power Sources 142(1):223–237
73. Tripathi BP, Shahi VK (2007) SPEEK–zirconium hydrogen phosphate composite membranes with low methanol permeability prepared by electro-migration and in situ precipitation. J Colloid Interface Sci 316(2):612–621
74. Lim SS, Wan Daud WR, Jahim J, Ghasemi M, Chong PS, Ismail M (2012) Sulfonated poly (ether ether ketone)/poly (ether sulfone) composite membranes as an alternative proton exchange membrane in microbial fuel cells. Int J Hydrogen Energy 37(15):11409–11424
75. Jiang Z, Zhao X, Manthiram A (2013) Sulfonated poly (ether ether ketone) membranes with sulfonated graphene oxide fillers for direct methanol fuel cells. Int J Hydrogen Energy 38 (14):5875–5884
76. Heo Y, Im H, Kim J (2013) The effect of sulfonated graphene oxide on sulfonated poly (ether ether ketone) membrane for direct methanol fuel cells. J Membr Sci 425:11–22
77. Wang J, Bai H, Zhang H, Zhao L, Yifan Li C (2015) Anhydrous proton exchange membrane of sulfonated poly (ether ether ketone) enabled by polydopamine-modified silica nanoparticles. Electrochim Acta 152:443–455
78. Gang M, He G, Li Z, Cao K, Li Z, Yin Y, Wu H, Jiang Z (2016) Graphitic carbon nitride nanosheets/sulfonated poly (ether ether ketone) nanocomposite membrane for direct methanol fuel cell application. J Membr Sci 507:1–11
79. Mossayebi Z, Saririchi T, Rowshanzamir S, Parnian MJ (2016) Investigation and optimization of physicochemical properties of sulfated zirconia/sulfonated poly (ether ether ketone) nanocomposite membranes for medium temperature proton exchange membrane fuel cells. Int J Hydrogen Energy 41(28):12293–12306

80. Rahnavard A, Rowshanzamir S, Parnian MJ, Amirkhanlou GR (2015) The effect of sulfonated poly (ether ether ketone) as the electrode ionomer for self-humidifying nanocomposite proton exchange membrane fuel cells. Energy 82:746–757
81. Salarizadeh P, Javanbhakht M, Abdollahi M, Naji L (2013) Preparation, characterization and properties of proton exchange nanocomposite membranes based on poly (vinyl alcohol) and poly (sulfonic acid)-grafted silica nanoparticles. Int J Hydrogen Energy 38(13):5473–5479
82. Liew C-W, Ramesh S, Arof A (2014) A novel approach on ionic liquid-based poly (vinyl alcohol) proton conductive polymer electrolytes for fuel cell applications. Int J Hydrogen Energy 39(6):2917–2928
83. Beydaghi H, Javanbakht M, Kowsari E (2014) Synthesis and characterization of poly (vinyl alcohol)/sulfonated graphene oxide nanocomposite membranes for use in proton exchange membrane fuel cells (PEMFCs). Ind Eng Chem Res 53(43):16621–16632
84. Mollá S, Compañ V (2015) Nanocomposite SPEEK-based membranes for direct methanol fuel cells at intermediate temperatures. J Membr Sci 492:123–136
85. Yang J-M, Wang N-C, Chiu H-C (2014) Preparation and characterization of poly (vinyl alcohol)/sodium alginate blended membrane for alkaline solid polymer electrolytes membrane. J Membr Sci 457:139–148
86. Huang C-Y, Lin J-S, Pan W-H, Shih C-M, Liu Y-L, Lue S-J (2016) Alkaline direct ethanol fuel cell performance using alkali-impregnated polyvinyl alcohol/functionalized carbon nano-tube solid electrolytes. J Power Sources 303:267–277